PRESENCE DETECTION AND TDOA ESTIMATION OF SPREAD SPECTRUM SIGNALS USING SENSOR ARRAY

Can UYSAL

Master of Science Thesis

Graduate School of Sciences
Electrical and Electronics Engineering Program

January 2015

This thesis work is supported in part by the Scientific Research Projects Commission of Anadolu University under the Master Thesis grant 1403F076.

JÜRİ VE ENSTİTÜ ONAYI

Can Uysal'ın **"Presence Detection and TDOA Estimation of Spread Spectrum Signals Using Sensor Array"** başlıklı **Elektrik-Elektronik Mühendisliği** Anabilim Dalı **Elektromanyetik Alanlar ve Mikrodalga Tekniği** Bilim Dalındaki Yüksek Lisans tezi 14 - 01 - 2015 tarihinde aşağıdaki jüri tarafından Anadolu Üniversitesi Lisansüstü Eğitim-Öğretim ve Sınav Yönetmeliğinin ilgili maddeleri uyarınca değerlendirilerek kabul edilmiştir.

	Adı -Soyadı	**İmza**
Üye (Danışman) :	**Yard.Doç.Dr. Tansu FİLİK**	.....
Üye :	**Prof.Dr. Ömer Nezih GEREK**	.....
Üye :	**Yard.Doç.Dr. Muzaffer DOĞAN**	.....

Anadolu Üniversitesi Fen Bilimleri Enstitüsü Yönetim Kurulu'nun ..... tarih ve ..... sayılı kararıyla onaylanmıştır.

Enstitü Müdürü

ABSTRACT

Master of Science Thesis

PRESENCE DETECTION AND TDOA ESTIMATION OF SPREAD SPECTRUM SIGNALS USING SENSOR ARRAY

Can Uysal

Anadolu University
Graduate School of Sciences
Electrical and Electronics Engineering Program

Supervisor : Assist.Prof.Dr. Tansu Filik

2015, 73 pages

In this thesis, the presence detection and time difference of arrival (TDOA) estimation of direct-sequence spread spectrum signals (DS-SS) in low signal to noise ratio (SNR) using the sensor array are considered. Two different methods are proposed for the presence detection of both the long and short code DS-SS signals. The first proposed method is based on the phase linearity of the cross channel terms of the spatial covariance ($\mathbf{R}$) matrices. The second detection method uses the eigenvalue ratios of the $\mathbf{R}$ matrices which is a known approach in literature. But to our knowledge this approach is firstly applied to long code DS-SS signals in this thesis. In addition, a new sample $\mathbf{R}$ matrix estimation technique, which is called as block of consecutive frequency bins (BCFB), is proposed. It is also shown that using the $\mathbf{R}$ matrix of the proposed BCFB method improves the detection performance especially in low SNR. In the second part of the thesis, TDOA of the received signals is also estimated using only the phase slope of the estimated $\mathbf{R}$ matrices in the first proposed detection method. In this way, by using the proposed presence detection method, it is also possible to estimate the TDOA between the sensors. In simulations, it is shown that the proposed TDOA estimators performance is efficient in low SNR and it attains to the Cramer Rao Lower Bound (CRLB).

Keywords: Spread spectrum; presence detection; sensor arrays; covariance matrices; phase linearity; TDOA estimation.

ÖZET

Yüksek Lisans Tezi

YAYILI SPEKTRUM SİNYALLERİN SENSOR DİZİLERİ İLE VARLIĞININ SAPTANMASI VE VZF KESTİRİMİ

Can Uysal

Anadolu Üniversitesi
Fen Bilimleri Enstitüsü
Elektrik-Elektronik Mühendisliği Anabilim Dalı

Danışman : Yard.Doç.Dr. Tansu Filik

2015, 73 sayfa

Bu tezde, sensör dizilerini kullanarak düşük sinyal/gürültü oranında (SNR), doğrudan sıralı yayılı spektrum sinyallerinin (DS-YS) varlığının saptanması ve varış zamanları farkının (VZF) kestirimi ele alınmıştır. Hem uzun hem de kısa kodlu DS-YS sinyallerinin varlığının saptanması için iki farklı yöntem önerilmiştir. İlk önerilen yöntem, uzaysal ilinti ($\mathbf{R}$) matrislerinin çapraz kanal elemanlarının faz doğrusallığına dayanmaktadır. İkinci yöntem literatürde bilinen bir yaklaşımdır ve $\mathbf{R}$ matrislerinin öz değer oranlarını kullanır. Ancak, bizim bilgimize göre bu yöntem uzun kod DS-YS sinyallerine ilk kez bu tezde uygulanmıştır. Bununla birlikte, ardışık frekans blokları (AFB) olarak adlandırılan, yeni bir örneklem $\mathbf{R}$ matrisi kestirim tekniği önerilmiştir. Ayrıca, önerilen AFB yöntemiyle kestirilen $\mathbf{R}$ matrisinin kullanılmasının özellikle düşük SNR'de saptama performansını iyileştirdiği gösterilmiştir. Tezin ikinci bölümünde, alınan sinyallerin VZF'si, ilk önerilen saptama yönteminde kestirilen $\mathbf{R}$ matrislerinin faz eğimleri kullanılarak kestirilmektedir. Böylece, önerilen varlık tespit yöntemini kullanarak sensörler arasındaki VZF'yi kestirmek de mümkün olmaktadır. Önerilen VZF kestiricilerinin performansının düşük SNR'de etkili olduğu ve Cramer Rao Alt Sınırına (CRLB)'a eriştiği simülasyonlarda gösterilmiştir.

Anahtar Kelimeler: Yayılı spektrum; sinyal tespiti; sensör dizileri; ilinti matrisleri; faz doğrusallığı; VZF kestirimi.

ACKNOWLEDGMENTS

I would like to express my special appreciation and thank sincerely to my supervisor Assist. Prof. Dr. Tansu Filik for his guidance, patience, support and encouragement. His motivation helped me in all the time of research and writing of this thesis.

I also would like to thank Prof. Dr. Ömer Nezih Gerek, and Assist. Prof. Dr. Muzaffer Doğan for serving in my committee.

I would like to thank TÜBİTAK for their financial support with scholarship during my master education, as well.

I would like to thank my family for their trust and support.

Finally, I want to thank my lovely wife Sultan Uysal for her unconditional support. Words cannot express how much I love her.

TABLE OF CONTENTS

LIST OF FIGURES

LIST OF TABLES

1. INTRODUCTION

1.1. Overview and Motivation

The thesis is about the presence detection and the time difference of arrival (TDOA) estimation of the spread spectrum signals using sensor array. Characteristics which make important this technique, are the low probability of intercept and anti-jamming capability [3]. The first patent in spread spectrum field was obtained by G. Guanella, considered as the inventor of spread spectrum technique, in 1938 [4]. During World War II, this technique was intensively used for the secure and privacy communication. In the following years, with the development of the technology, number of applications had been actualized. Some of these applications improved in USA are given in the following. JTIDS (Joint Tactical Information Distribution System) was developed by DoD (Development of Defense) with the aim of secure and jamming resistant communication and navigation [5]. Global Positioning System, GPS, a worldwide navigation system, was improved to localize the objects on the face of the earth accurately. This system had been utilized in military applications up to 1980s [6]. TDRSS (Tracking and Data Relay Satellite System) using spread spectrum technology was developed by NASA to ensure ranging and communication for the low-earth orbiting satellites. In 1960s and 1970s, the studies of the scientists such as G. Solomon, R. Gold, T. Kasami etc., shaped the spread spectrum technology substantially [4]. In these years, many studies were published in that field [7–11]. Up to end of 1970s, spread spectrum technologies had been developed heavily by the military institutions and drowned in secrecy. In the following years, the spread spectrum techniques began to be used for commercial purposes [12]. Code division multiple access technique which employs spread spectrum technology, had been used in military applications previously and it started to be developed commercially. In the beginning of the 1990s, as well as the personal wireless communication came up, the spread spectrum method gained a seat in this field and provided

a basis for mobile cellular communication standards like IS-95, GSM. Recently, spread spectrum techniques are used in applications such as personal communications, cellular telephony, wireless alarm systems, local-area networks, short range telemetry and paging systems [12].

Spread spectrum signals provide secure and privacy communication as they are low probability of intercept signals. For this reason they are commonly used in military applications. Therefore, presence detection of hostile signals is very crucial in military communication and it becomes up-to-date research topic. Firstly, common detection methods were based on energy detection [13]. This methods measure the signal energy in specific time intervals and decide the presence or absence of the signal [14]. With the developing of spread spectrum technology, energy measurement based methods (radiometer) became useless [15,16]. They were badly affected by the changing of noise level because of depending on the noise power. Likewise they were also indurable against interferences. Subsequently, new methods using cyclic feature of the communication signal, have emerged [17]. This cyclic feature detectors exploit the cyclostationary properties of the signal such as carrier frequency [18], chip period [19] and spread sequence period [20]. If the autocorrelation function of any zero mean process changes periodically in time, this signal can be defined as cyclostationary [21]. Besides these, there are many studies using cyclostationary properties of spread spectrum signals [22, 23]. But this methods do not work for the long-code spread spectrum signals where the period of the spreading sequence is quite larger than the symbol period. The above property of the long spreading codes destroys the symbol-interval cyclostationary properties of the transmitted signal [24].

In literature, the studies on the detection of long-code spread spectrum signals is not as rich as the studies on the short code signals. Some studies concerning long-code signals are given in [25–28]. In [27], a spreading sequence estimation algorithm is presented. This algorithm is the improved version of the study in [22] and it is developed for the long code signals. In [28], in order to estimate the spreading waveform of the long-code DS-SS signals, a

missing data model based method is proposed. The long-code DS-SS signal is represented as a short code DS-SS signal in this data model. In [25], a performance analysis of the long-code DS-SS signals is given in the presence of various interferences. The main idea in this work is to evaluate the symbol error probability. The detection methods proposed in this thesis, can detect both the short and long code spread spectrum signals. There are some other studies based on higher order statistics [29–31], time-frequency analysis [32] in literature. Eigenanalysis in spread spectrum technique is commonly used for interference rejection [33], parameter estimation [34] and synchronization [35] not for the multichannel signal detection. In literature, spread spectrum signal detection methods detect the signal over a single channel. There is a multichannel method in [36] but the used algorithm and performance details are not clear. In this thesis, two different multichannel detection methods are proposed for the detection of spread spectrum signals.

The presence detection and TDOA estimation of the spread spectrum signals are crucial and challenging problems currently. The motivation of this thesis comes from the presence detection of long code spread spectrum signals is a open problem and there is no detection method in literature. Existing presence detection methods are not effective in low SNR. Also, in the practical real time applications, a computationally efficient presence detection method is needed. In this thesis, it is aimed to propose novel multichannel presence detection methods. In addition, the TDOA between the sensors can be estimated using the estimated phase slope in the detection method.

1.2. Thesis Outline

The outline of the thesis is given below:

In Chapter 2, the background informations for spread spectrum technique are given. The basic principles, advantages and the most commonly used types of spread spectrum technique are presented.

In Chapter 3, two different multichannel methods are proposed for the presence detection of both the long and short code DS-SS signals. The basic

principles of DS-SS signals is summarized in Section 3.1. Then the properties and the types of the spreading code which is a key parameter for the spread spectrum signals, are described in Section 3.2. Afterwards, the signal model and problem formulation are given in Section 3.3. The presence detection methods for the DS-SS signals are proposed in Section 3.4 and 3.5. In addition, a new sample spatial covariance matrix ($\mathbf{R}$) estimation technique, which is called as block of consecutive frequency bins (BCFB), is proposed in section 3.5. Finally, the detection performances of the proposed methods are given in the various simulations.

In Chapter 4, time delay estimation problem is considered. In Section 4.1, for TDOA estimation, the previous studies in literature are discussed. The data model is given in Section 4.2. The frequency domain TDOA estimator is proposed in Section 4.3. Finally, the simulation results show the proposed estimator can estimate the TDOA in quite low SNR and it attains to the CRLB.

In Chapter 5, the conclusion of the thesis is given.

1.3. Contributions

In this thesis, two different multichannel methods are proposed for the presence detection of both the long and short code DS-SS signals. The main contributions of the thesis are stated in two parts as below:

1- The presence signal detection methods:

a-) Proposed Method I:

- The proposed method uses the linearity of phase slope between the cross channels of the covariance matrices [37].
- The method is able to detect both the short and long code spread spectrum (SS) signals in low SNR.

b-) Proposed Method II:

- A simple and efficient method uses the eigenvalue ratios of the covariance matrices [38].

- A new sample spatial covariance matrix ($\mathbf{R}$) estimation technique, which is called as block of consecutive frequency bins (BCFB), is proposed.
- The proposed method can also detect both the short and long code DS-SS signals in low SNR.

2- The proposed TDOA estimation method:

- TDOA of the received signals is estimated using only the phase slope of the estimated R matrices in the proposed detection method I.
- The sample covariance matrices are also estimated using BCFB explained in the proposed detection method II.

2. SPREAD SPECTRUM SIGNALS

Spread spectrum is a transmission technique and its main principle is to transmit information signal with a greater bandwidth than the present bandwidth [3]. This spreading operation is implemented by multiplying information signal with a higher frequency Pseudo-Random (PN) code which is noise like and independent from the signal [6]. As the information signal is spread over a wider band and transmitted below the noise level, this technique is secure and resistant to jamming, interferences.

Let's tackle two basic models of jammer: Narrowband and barrage jammer. The bandwidth of the narrowband jammer is quite smaller than the spread signals bandwidth. So, the narrowband jammer corrupts the partial-band of the spread signal, and this can be eliminated by using band-elimination filter or shifting signal spectrum to the free zones. In the second case, the barrage jammer, which covers the whole spectrum, is used to jam a hostile signal. In this situation, as the power of the jammer is spread over a wider band, its effect on the signal decreases. Thus, it can be said that the spread spectrum technique has an anti-jamming capability [4].

The interception of hostile communications is an essential and preferential case in communications. Typically, the interceptor keeps the frequency spectrum under surveillance and measures the transmitted power (this technique is called energy detector). As the spread spectrum communication systems operates with low radiated power, the transmitted signal is hidden into the noise. Because of this properties, spread spectrum signals are named as low probability of intercept (LPI) signals [39].

Unlike the other multiple access techniques, the spread spectrum systems provide multiple transmitters to share the frequency spectrum at the same time by using unique code sequences. This technique does not require sharing of the frequency band and time synchronization of the users. Here, each user is assigned a code, thus they do not interfere with the each other. Without the spreading code sequence, recovering the spread spectrum signal

is not possible. Thereby, this technique provides secure and confidential communication to the individual users even in the presence of the other users in the frequency spectrum.

In multipath fading case, the transmitted signal can arrive at the receiver via different paths. Signals can reflect from various objects and atmosphere e.g., buildings, towers, air crafts and others as seen in the Figure 2.1.

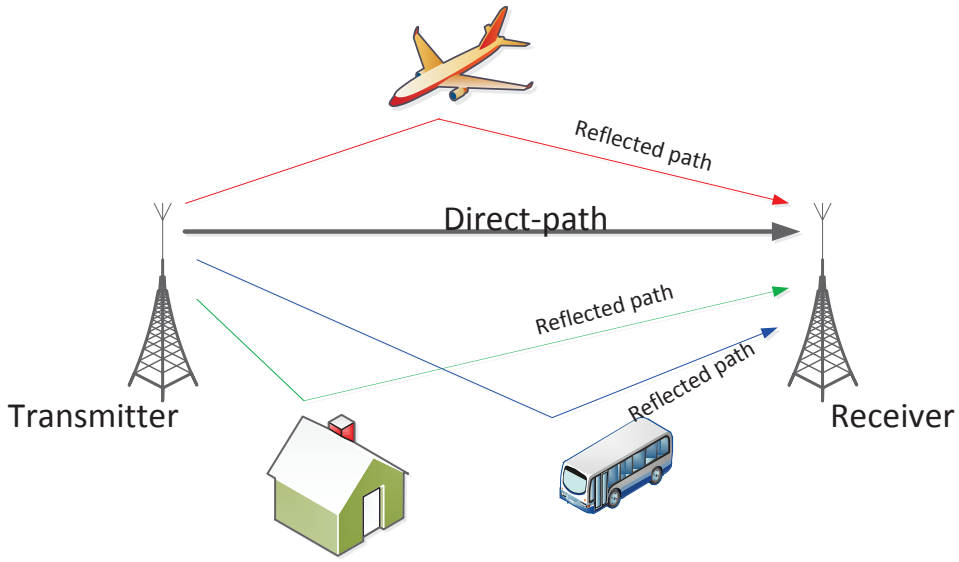

Figure 2.1.: Scheme of the multipath propagation.

When the spreading code multiplies by its asynchronous replica, the result will have a very low value. Since the receiver is synchronous only with the direct-path signal, it perceives all of the other multipath signals as a noise. The merits of the spread spectrum systems are given as below,

- Anti-jamming and anti-interference
- Low probability of intercept
- Resistance to multipath fading
- Secure and confidential communication

- Low power spectral density
- Multiple access

The most commonly used types of spread spectrum techniques are Frequency Hopping Spread Spectrum (FH-SS) and Direct Sequence Spread Spectrum (DS-SS) [1].

2.1. Frequency Hopping Spread Spectrum

The carrier frequency of the transmitted signal hops periodically between the available frequencies in the frequency hopping schedule. This operation is called Frequency Hopping (FH). Typically, data modulation is frequency-shift keying (FSK) in frequency hopping systems [40]. The carrier frequency hops according to the pseudo-random phases of the spread spectrum sequence at the transmitter. The hopping frequency range is wider than the information signal bandwidth. The time duration between the frequency hops is called the hop period, T_h, and the bit period of the information data is denoted by T_b. According to the relation between the hop period and the bit period, FH systems are classified into two types: Fast and slow frequency hopping.

$$T_h \leq T_b \longrightarrow Fast\,FH$$

$$T_h > T_b \longrightarrow Slow\,FH$$

In other words, in fast FH system, a data symbol is transmitted with several frequency hops. On the other hand, during one frequency hop, several data symbols may be transmitted in slow FH systems. Even if fast FH has some advantages to slow FH, is not preferred in practice because of its difficult implementation [1].

At the FH receiver, the signal filtered with a wideband bandpass filter is multiplied with an identical FH carrier. Then the output signal is filtered again and applied to the appropriate demodulator. It should be noted that the spreading code sequence used at the receiver must be synchronous with the one at the transmitter in order to recover the information data correctly.

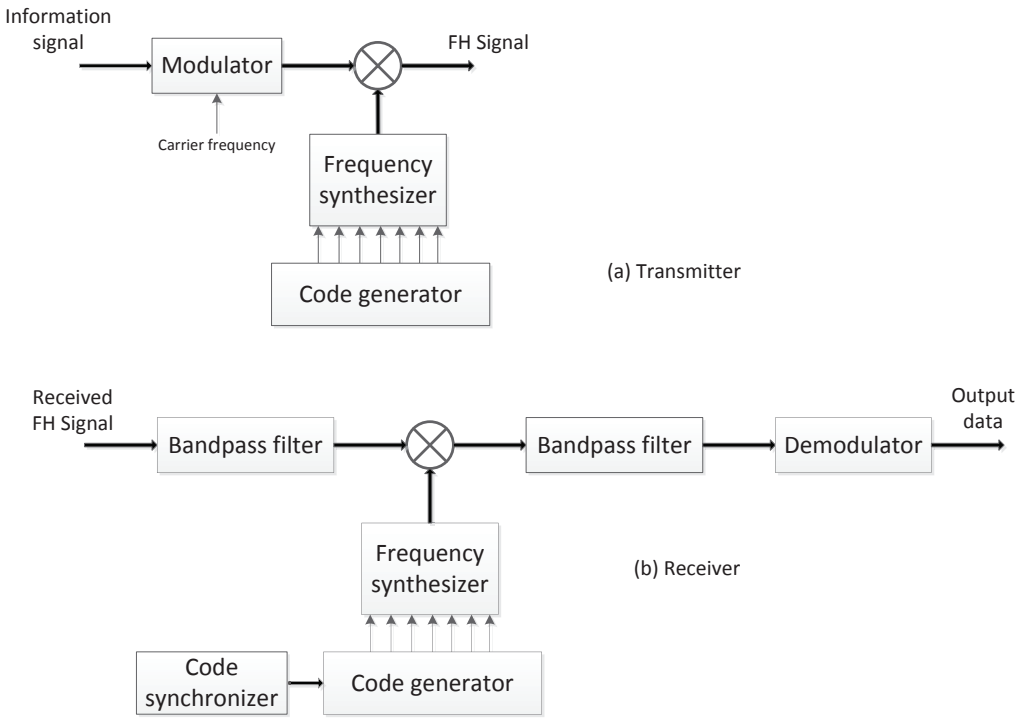

Figure 2.2.: Block diagram of FH transmitter (a) and receiver (b) [1].

2.2. Direct Sequence Spread Spectrum

As similar with the basic idea of the spread spectrum, direct sequence system expands the information signal bandwidth. Not only the signal bandwidth is expanded, the transmitter power is also spread with a low power spectral density [4].

In this technique, the information data is 'directly' multiplied with a spreading code sequence before the final carrier modulation at the transmitter [41]. Then, the received signal is multiplied again with the same spreading code at the receiver in order to recover the original signal. As is understood from this process, when the spreading code is multiplied by its own, it is expected to lose its effect. For this reason, spreading codes consist of '+1's and '-1's. Thus, the result of multiplication of the spreading code by itself always will be '1'.

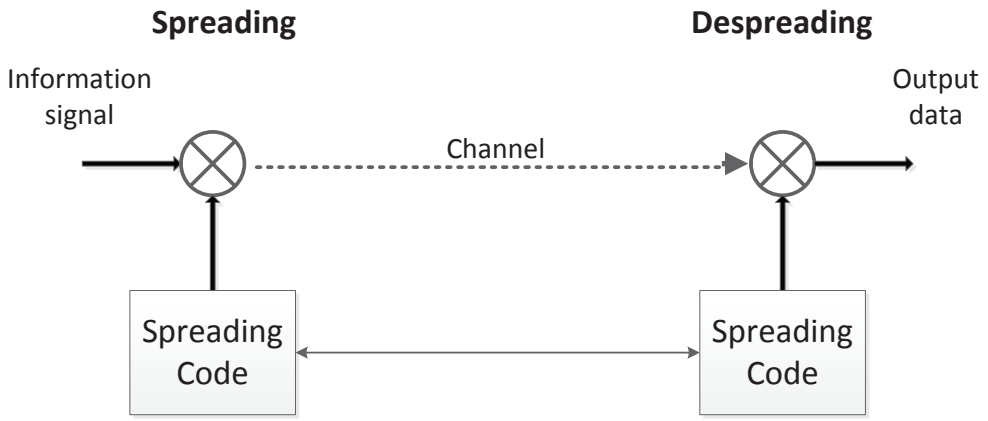

Figure 2.3.: The spreading and despreading operations.

Figure 2.3. shows the spreading and despreading operations. Here, T_c is the chip duration and T_s denotes the symbol duration of the data. N is the length of the spreading sequence. R_c and R_s represents chip rate and symbol rate respectively. It is seen in the figure, bandwidth of the spread spectrum signal is much greater than the bandwidth of the information signal ($BW_{info} = R_s \ll BW_{ss} = R_c$). The bandwidth expansion factor which is called spreading factor is given as below,

$$SF = G_p = \frac{BW_{ss}}{BW_{info}} = \frac{R_c}{R_s} = \frac{T_s}{T_c} = N$$

where, G_p is the processing gain and it equals the ratio between chip rate and symbol rate.

DS-SS signals can be classified into two types according to the relationship between the symbol duration (bit period) and the period of the spreading sequence: The long-code (LC) and the short-code (SC) signals [28]. In the SC systems, the bit period of the signal equals to the multiplication of spreading factor and chip duration. In the LC systems, the period of the spreading sequence is larger than the symbol duration [27, 42]. In other words, spreading factor is larger than the length of the spreading sequence in the LC

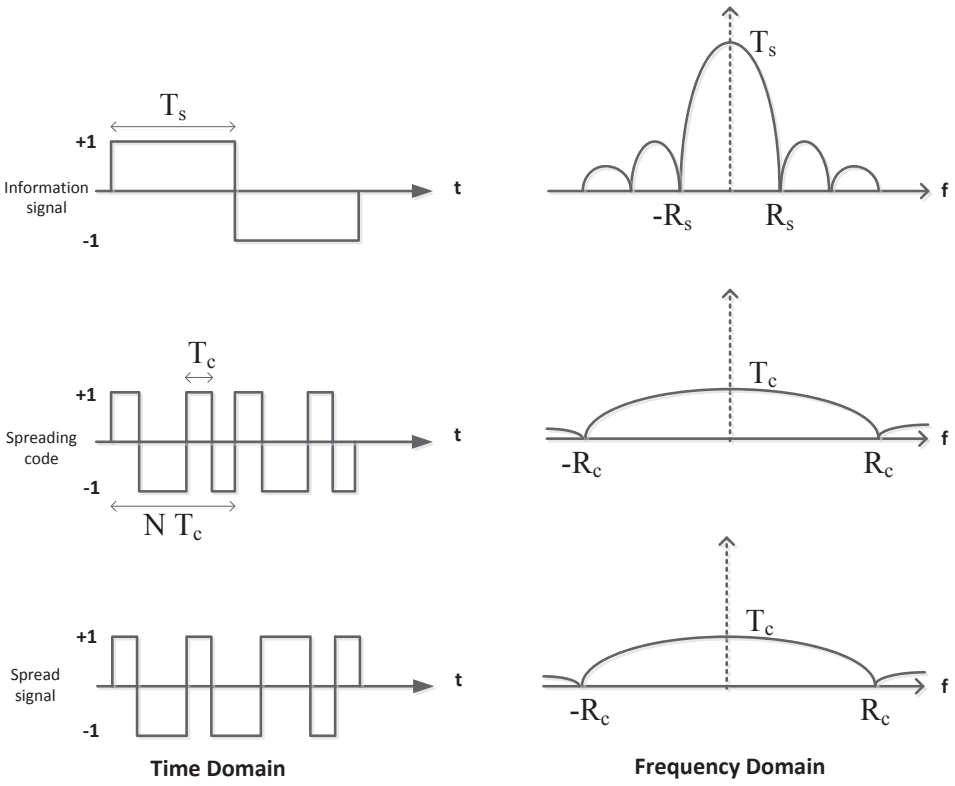

Figure 2.4.: Spreading scheme in time and frequency domain.

systems. While a spreading sequence is associated with one data symbol in a SC system, it corresponds to more than one symbol in a LC system. Scheme of the short and the long code spread signals are given in Figure 2.5..

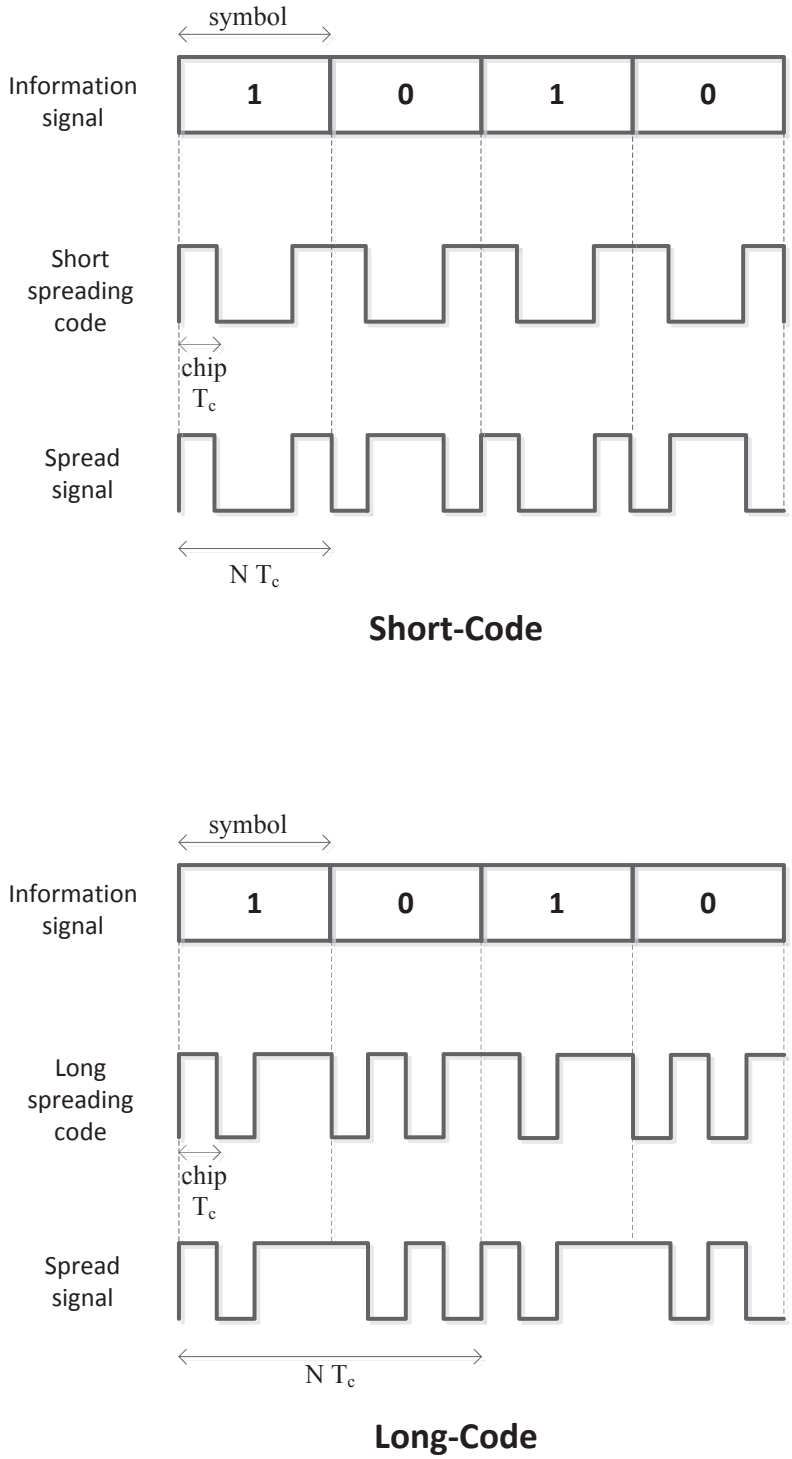

Figure 2.5.: Scheme of the short and long code spread signals.

3. PRESENCE DETECTION OF SPREAD SPECTRUM SIGNALS

In this chapter, the basic principle of DS-SS signals is summarized firstly. Besides a transmission system including a transmitter, a receiver and a signal detector is figured in the first section. Then the properties and the types of the spreading code which is key parameter for the spread spectrum signals, are described. Afterwards, the signal model and problem formulation are given. Finally, implemented two method for the presence detection of DS-SS signals are investigated.

3.1. Introduction

DS-SS signals are usually preferred for secure wireless communications in military applications and also in civilian applications such as Global Positioning System (GPS), Code Division Multiple Access (CDMA) [6]. DS-SS signals are also resistant to narrowband interference, noise and jamming. Furthermore, spread spectrum communications limit the energy consumption and especially preferred in satellite downlinks. The main principle of spreading the signals is to transmit information data with a larger bandwidth than the present bandwidth. This spreading operation is implemented by multiplying data with a higher frequency Pseudo-Random number (PN) code which is noise-like and independent from data. The non-cooperative presence detection of DS-SS signals in low SNR is challenging and important problem for the applications such as spectrum surveillance, source localization, etc. and widely studies in literature [43]. Most of these detection methods are based on the repeating structure of the spreading code (which is also called as Pseudo-noise (PN)). Whereas for the very long code DS-SS signals, whose spreading code length is larger than the spreading factor, the length of codes are on the order of days, the cyclostationary properties of these signals are destroyed [24] and the most of the proposed methods in literature are useless . Since these signals are spread in wide frequency band and transmitted below noise level, wideband array signal processing techniques are more suitable for detection and

parameter estimation. In this thesis, two different methods are proposed for the presence detection of both the short and long-code DS-SS signals, which are based on wideband array signal processing. The first proposed method is a multichannel detection method which uses phase linearity between the spatial covariances of the cross sensors. In the second proposed method, a simple and computationally efficient two channel presence detection system which based on the eigenvalue ratios of the sample spatial covariance matrices is proposed. A transmission scheme for the DS-SS system is shown in Figure

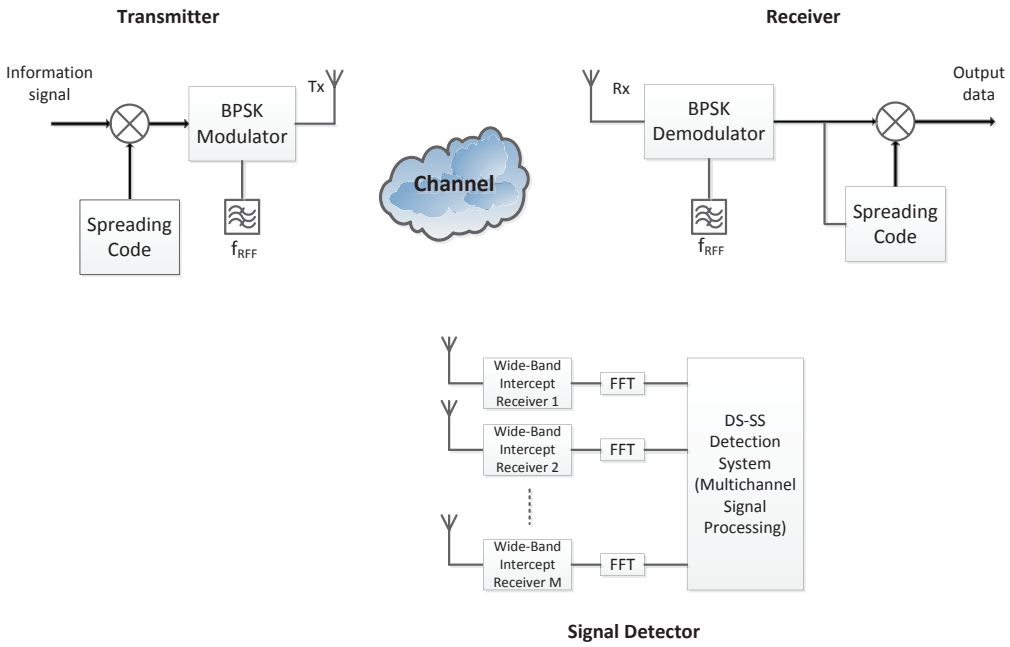

Figure 3.1.: A DS-SS transmission scenario.

3.1. Here, a transmitter, a receiver and multichannel detection system are seen in the figure. In DS-SS systems, the data signal is spread by multiplying with higher frequency PN Code as shown in the figure. Then the spread signal is modulated to a reference frequency with a BPSK (Binary Phase Shift Keying) modulator. PN codes have a great importance in DS-SS systems. The signal is spread in the transmitter and despread in the receiver by PN codes. These codes seem random but they are generated according to certain rules which

will be described in the following section [39]. Non-cooperative multichannel DS-SS detection system collects the signals with spatially distributed array of M sensors as in Figure 3.1.

3.2. Spreading Codes

Spreading codes (PN, Pseudo-Noise) are very crucial parameter for spread spectrum signals [41]. As mentioned in the previous chapters, information signal is directly multiplied by the spreading code in spread spectrum technique. Thus, while the bandwidth of the signal expands, the power density of the signal decreases. For an efficient transmission, PN sequence must be different from the other PN sequences or its time shifted version. Accordingly, to enable many users to share frequency spectrum without interference, spreading codes must be selected carefully.

In cooperative spread spectrum communications, PN sequences are known in both the transmitter and the receiver. Otherwise, the receiver has no chance to despread the signal. PN codes are noise-like and they seem to be random from the outside. But actually they are periodic. The spreading sequences are formed according to some specific features [39]. The properties of the spreading codes are given in the following.

3.2.1. Properties of the Spreading Codes

There are some important properties of the binary spreading sequences.

- **Balance Property:** The number of +1s of spreading code in each period should be one more than the number of -1s.

$$PN = 1 \quad 1 \quad -1 \quad 1 \quad -1 \quad -1 \quad 1 \quad \longrightarrow \sum = 1$$

- **Run Property:** A run is a subsequence of a single type of symbols. Symbol number in a run states the length of the run. In a sequence, the length of the half of the total run number is 1, the length of one fourth is 2, and the length of one eighth is 3...

- **Correlation Property:** PN sequences have some correlation properties. These are;

- Autocorrelation: It is similarity between a signal and its own or its time shifted version.

$$R_a(\tau) = \frac{1}{NT_c} \int_{-\frac{NT_c}{2}}^{\frac{NT_c}{2}} pn(t)\ pn(t-\tau)dt \tag{3.1}$$

$$R_a(\tau) = \begin{cases} 1, & \tau=0,\ NT_c,\ 2NT_c.. \\ -\frac{1}{NT_c}, & otherwise \end{cases} \tag{3.2}$$

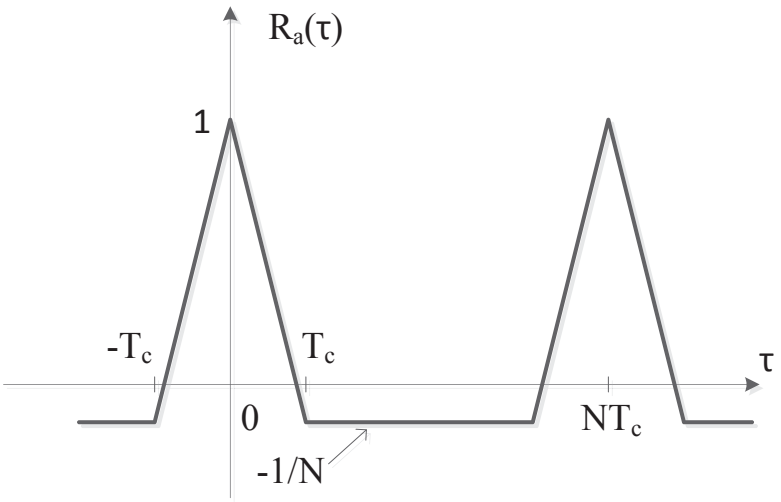

Figure 3.2.: Autocorrelation function of a spreading code.

If the spreading sequence is periodic, its autocorrelation function is also periodic with the length of the spreading sequence, N. As it seen in Figure 3.2., the autocorrelation function of the signal peaks only where two sequences are correlated with each other. In spread spectrum communication, the synchronization between the transmitter and the receiver is provided by this feature. Thus, that despreads the received signal correctly. In the absence of synchronization, only noise can be obtained.

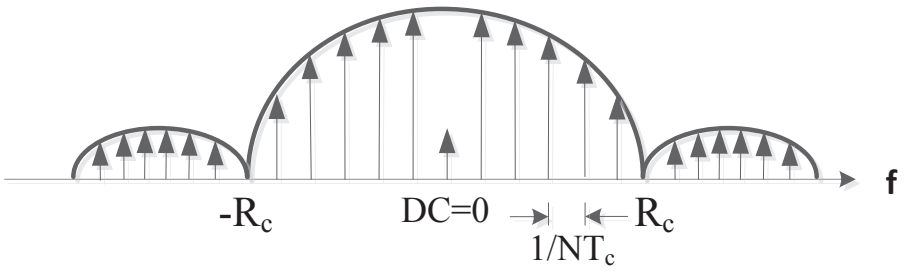

Figure 3.3.: Power spectral density of a spreading code.

- Cross correlation: It is the measurement of similarity between two different signals. In the case of dissimilarity between the spreading codes, the cross correlation function takes too small value. Such codes are called as orthogonal. Especially in the multiple access applications, if the user codes are orthogonal, the receiver can distinguish the information came from different users, and the privacy in communication is emerged. Otherwise, interference between the users increase and signals begin to be affected by each other.

$$R_c(\tau) = \frac{1}{NT_c} \int_{-\frac{NT_c}{2}}^{\frac{NT_c}{2}} pn_1(t)\ pn_2(t-\tau)dt \tag{3.3}$$

3.2.2. Types of Spreading Code

There are some common types of the spreading codes:

Maximum Length Sequence (M-sequence): This sequences are the most common type of the spreading codes used in spread spectrum systems. They are also called as M-sequences. In general, they are used in single-user applications. M-sequences have all above properties of the spreading codes. Linear

feedback register circuits and modulo-2 adders are used in order to generate m-sequences.

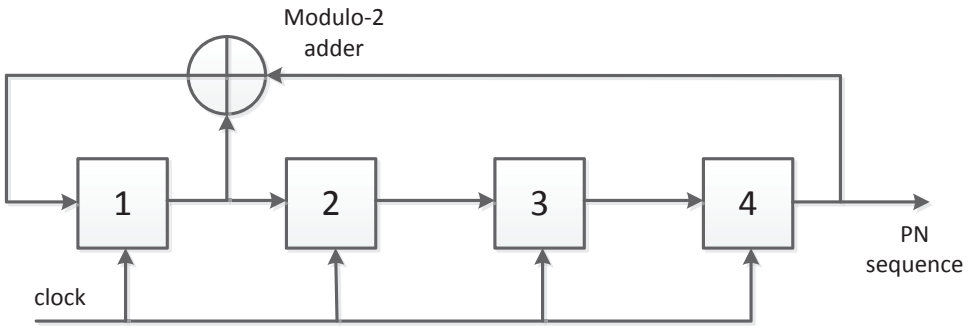

Figure 3.4.: M-sequence generator scheme [2]

A simple m-sequence generator is shown in Figure 3.4. The period of the sequence is $N = 2m-1$, where m is the number of registers. Initial state is crucial for the periodic cycle of the states [3]. For example, if the initial value is 1111, the m-sequence will be 111101011001000. This sequence has the all characteristics of the spreading codes. The N states indicate the N different stages of the m-sequences. Another property of m-sequence is that, modulo-2 summation of the m-sequence and its any shifted phase gives a different phase of the same m-sequence.

Gold Codes: These codes are generated with modulo-2 summation of the preferred pairs of m-sequences in the same length, as seen in the Figure 3.5. A pair of m-sequences, which have a cross correlation limited with three values, are called preferred pairs [39]. As they have lower cross correlation values than m-sequences, they are preferred in the multiple user CDMA systems. Depending on rapid synchronization, secure communication and good cross correlation properties, Gold codes are commonly used in GPS systems [2].

Hadamard-Walsh Codes: Totally, there are $N = 2n$ codes in the length of N.

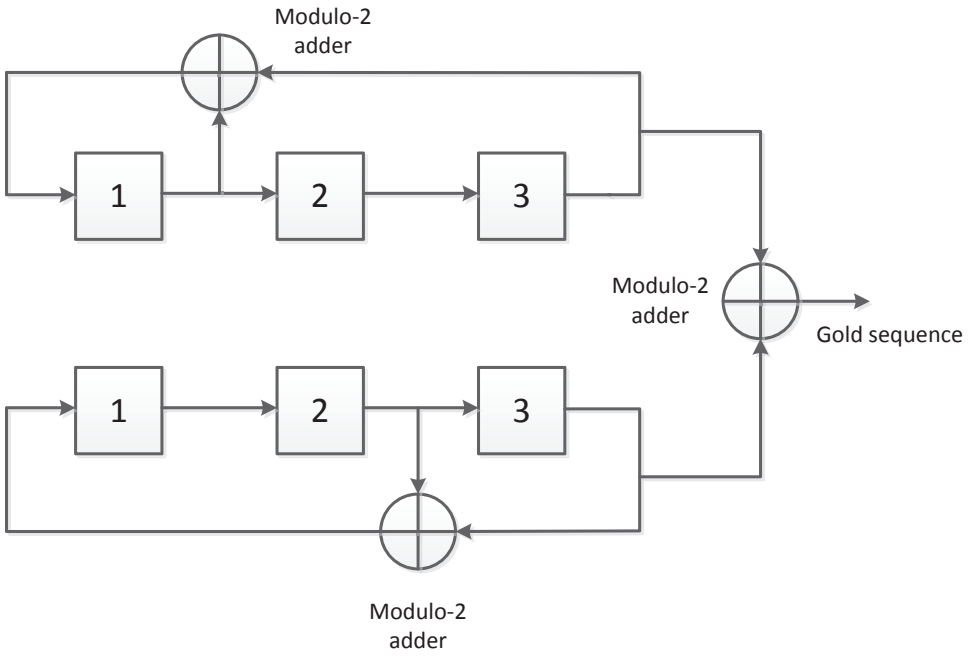

Figure 3.5.: Scheme of the generation of Gold Codes.

$$H_N = \begin{bmatrix} H_{N/2} & H_{N/2} \\ H_{N/2} & -H_{N/2} \end{bmatrix} \; with \; H_1 = [1]$$

Walsh codes are generated from Hadamard matrices and they are also called as Hadamard-Walsh Codes . Each row or column in Hadamard matrix corresponds to a Walsh code sequence in n length [39]. Owing to the orthogonality between the codes, their cross correlation values become zero. This situation prevents the interference between the signals using the same band in CDMA systems. In Hadamard matrix, $\frac{N}{2}$ elements of each row (or column) are different from another row (or column).

3.3. Signal Model and Problem Formulation

General signal detection problem with binary hypothesis test is expressed below,

$$\begin{aligned} H_0 &: y_m[n] = w_m[n], && n = 1, ..., N \\ H_1 &: y_m[n] = s_m[n] + w_m[n], && m = 1, ..., M \end{aligned} \tag{3.4}$$

Here, H_0 and H_1 are cases of the absence of signal and the presence of signal, respectively. N is the number of samples collected from each receiver. It is assumed that the noise, $w[n]$ is temporally and spatially uncorrelated, white, zero mean Gaussian and has σ^2 variance. For the H_1 case, the multichannel DS-SS detection system collects the signals with spatially distributed array of M sensors as in Figure 3.1. The received DS-SS signal by m^{th} sensor is modelled as,

$$y_m[n] = \underbrace{x[n - \Delta_m]c[n - \Delta_m]}_{s[n-\Delta_m]} + w_m[n] \tag{3.5}$$

where m is sensor index, Δ_m is time shift between m^{th} sensor and reference sensor, $x[n]$ is the source signal, $c[n]$ is long spreading code with length of L. For the long-code DS-SS signals, L is larger than the spreading factor [28]. In multipath case, the received signal is expressed as,

$$y_m[n] = \sum_{p=1}^{P} \alpha_{mp} s[n - \Delta_{mp}] + w_m[n] \tag{3.6}$$

where α_{mp} is the attenuation factor in the p^{th} path to the m^{th} sensor. P is the number of paths, Δ_{mp} is the time delay between m^{th} sensor and reference sensor for p^{th} path. For the ideal propagation model, frequency domain expression of (3.5) is,

$$Y_m[k] = e^{-j2\pi k\Delta_m/K} \underbrace{(X[k] \otimes C[k])}_{S[k]} + W_m[k], \qquad k = 1, ..., K \tag{3.7}$$

where k is the index of frequency bin, K is the total number of frequency bins ($K \leq N$) and $\otimes$ denotes convolution. The sensor output vector of M sensors

in frequency domain is given as,

$$\mathbf{Y}[k] = \mathbf{A}[k]S[k] + \mathbf{W}[k], \qquad k = 1, ..., K \tag{3.8}$$

The wideband spatial covariance matrix of k^{th} frequency bin is defined as,

$$\mathbf{R}[k] = E\{\mathbf{Y}[k]\mathbf{Y}^H[k]\} \tag{3.9}$$

$$\mathbf{R}[k] = \mathbf{A}[k]R_s[k]\mathbf{A}^H[k] + \sigma^2\mathbf{I}[k] \tag{3.10}$$

where $(.)^H$ denotes the conjugate transpose of a matrix, $\mathbf{A}[k]$ is the manifold vector and $\mathbf{I}[k]$ is the identity matrix. It is assumed that, there is a single wideband signal, $S[k]$, and the signal covariance is,

$$R_s[k] = E\{S[k]S^H[k]\} \tag{3.11}$$

3.4. Detection of DS-SS Signal Based on Phase Linearity

DS-SS signals are noise-like signals and are transmitted below the noise level. If the wideband DS-SS signal is present, as the propagation velocity of the source signal $x[n]$ is constant, the phase response of wideband cross channel covariance terms will be linear along the signal bandwidth [44]. In the presence of the signal, the amplitude and phase response of one of the cross channel terms are given in Figure 3.6. and Figure 3.7. respectively. On the contrary, in noise only case, the phase response of the covariance matrix cross elements is far from the linearity as shown in Figure 3.8.

In this section, a method which uses the linearity of the phase response of the wideband spatial covariance matrix cross elements of sensor arrays, is proposed. The steps of this proposed method is given in the following section.

In wideband signal processing, wideband signals are decomposed into many narrowband signals using Discrete Fourier Transform (DFT) in order to apply narrowband techniques to the wideband signals [45]. Then, the narrowband frequency components are processed separately and the final estimate is averaged over all the frequency components. The steps of this approach are summarized below.

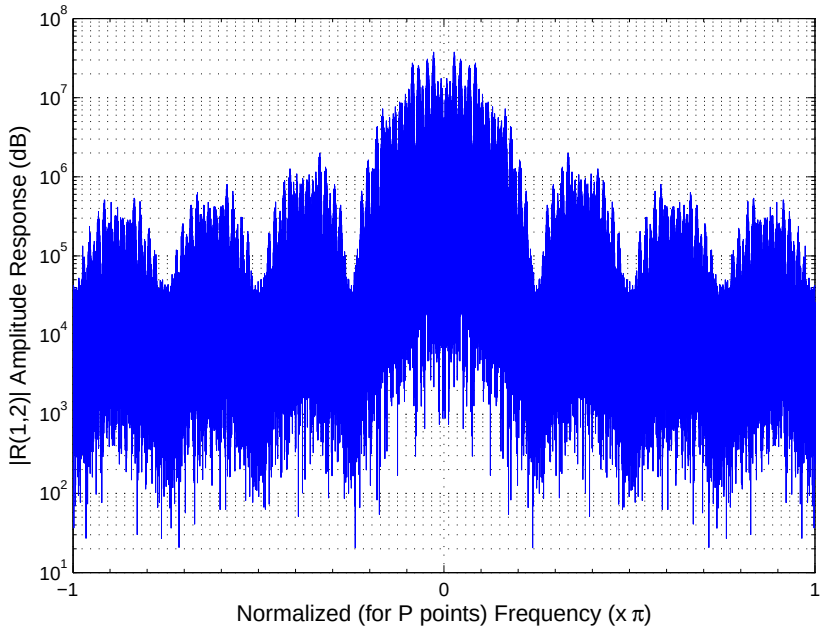

Figure 3.6.: The amplitude response of wideband cross channel covariance terms (R (1, 2)) in the presence of a signal.

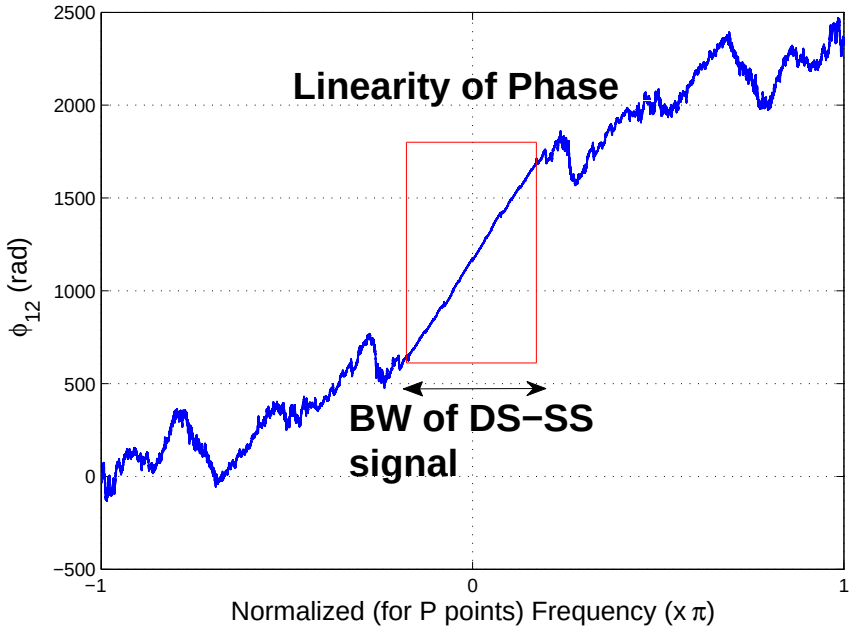

Figure 3.7.: The phase response of wideband cross channel covariance terms (R (1, 2)) in the presence of a signal.

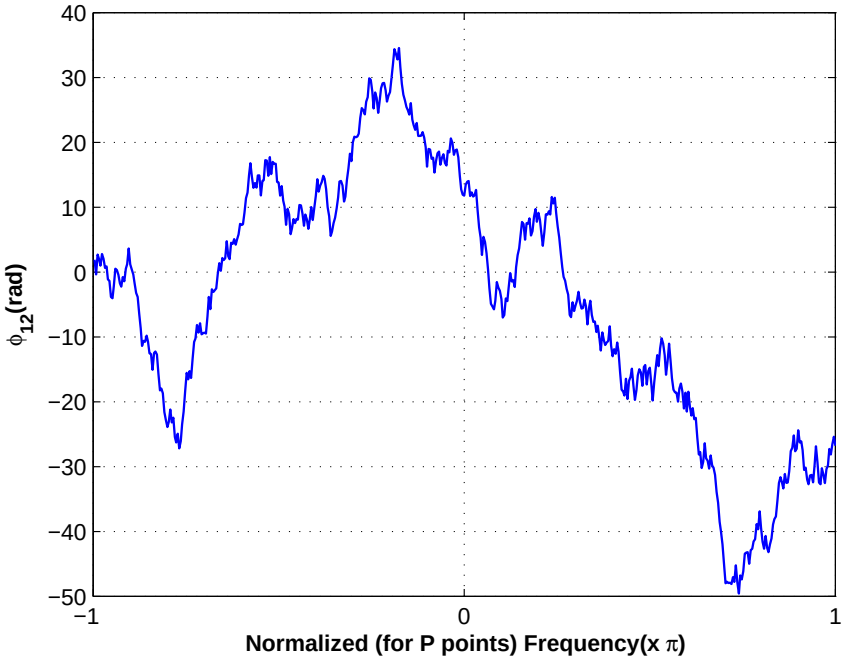

Figure 3.8.: The phase response of wideband cross channel covariance terms (R (1, 2)) in noise only case.

- Wideband signal is divided equally into non-overlapping B snapshots.
- The temporal Discrete Fourier Transform (DFT) of the B snapshots is computed and spatial covariance matrices are estimated as below,

$$\hat{\mathbf{R}}_p = \frac{1}{B}\sum_{b=1}^{B} \mathbf{Y}_{b,p}\mathbf{Y}_{b,p}^H \qquad \substack{p=1,\ldots,P \\ b=1,\ldots,B} \tag{3.12}$$

where, B is the total number of snapshots and P is the number of frequency bins in each snapshot. $Y_{b,p}$ represents b^{th} snapshot and the p^{th} frequency component of the sensors output. Furthermore, $\hat{\mathbf{R}}_p$ is an $M \times M$ matrix and there are total P covariance matrices. For the p^{th} frequency bin, the phase value of the cross terms of $\hat{\mathbf{R}}_p$ is given as,

$$\phi_p(i,j) = arg(\hat{\mathbf{R}}_p(i,j)), \qquad \substack{p=1,\ldots,P \\ i=1,..,M-1, \\ i<j} \quad \substack{ \\ j=2,..,M} \tag{3.13}$$

where i is the row and j is the column index of the matrix in (3.12). Accordingly, $\phi_{p(i,j)}$ is computed for P frequency components and the phase response is obtained with the combining all the estimated phase values. The phase response of the first and second wideband cross channel covariance terms is shown in Figure 3.7. As seen in figure, in the presence of a signal, the phase response has linear characteristics along the bandwidth of the signal. As well as being slope differences, there is also a linearity in the phase responses of other cross terms. A straight line is fitted to the phase response throughout F frequency bins by using a linear model which is defined as,

$$\phi_f(i,j) = \alpha(i,j) + \beta(i,j)f, \quad f = \frac{P-F}{2} + 1, ..., \frac{P+F}{2} \tag{3.14}$$

where f is the frequency bin index, $\alpha(i,j)$ is an initial (intercept) point and $\beta(i,j)$ is the slope of the fitted line. The F frequency bins ($F < P$) which should be in the bandwidth of the signal are chosen symmetrically from the both sides of center frequency of the signal. The model in (3.14) can be expressed for each i^{th}, j^{th} cross terms in covariance matrix form as,

$$\mathbf{v}(i,j) = \mathbf{H}\boldsymbol{\theta}(i,j) + \mathbf{w} \tag{3.15}$$

where $\mathbf{v}(i,j) = \left[\phi_{\frac{P-F}{2}+1}(i,j) \dots \phi_{\frac{P+F}{2}}(i,j)\right]^T$ is the observed data set and $\mathbf{w} = \left[w_{\frac{P-F}{2}+1} \dots w_{\frac{P+F}{2}}\right]^T$ is the unknown noise which represents the deviation from the model. $\mathbf{H}$ is the known observation matrix,

$$\mathbf{H} = \begin{bmatrix} 1 & \frac{P-F}{2}+1 \\ \vdots & \vdots \\ 1 & \frac{P+F}{2} \end{bmatrix}_{\mathbf{F\times 2}} \tag{3.16}$$

and finally $\boldsymbol{\theta}(i,j)$ is the unknown parameter vector $\boldsymbol{\theta}(i,j) = [\alpha(i,j)\ \beta(i,j)]^T$. Hence, the parameters of the fitted lines for each cross terms of (3.12) can be estimated as,

$$\hat{\boldsymbol{\theta}}(i,j) = (\mathbf{H^T H})^{-1}\mathbf{H^T}\mathbf{v}(i,j) \tag{3.17}$$

which is the minimum variance unbiased estimator for the given model in (3.15). Thus, the estimated coefficients in (3.17) are the optimum line parameters of $\hat{\phi}_f(i,j) = \hat{\alpha}(i,j) + \hat{\beta}(i,j)f$.

3.4.1. Detection Algorithm

- **Step 1:** Measure the total difference between the phase response and the optimum fitted lines for all cross channel terms. In order to measure the difference, we use normalized total root mean square error, $Total_{RMSE}$ is,

$$Total_{RMSE} = \sqrt{\frac{2}{M(M-1)F} \sum_{\substack{i=1 \\ i<j}}^{M-1} \sum_{\substack{j=2 \\ i \neq j}}^{M} \sum_{f=1}^{F} (\phi_f(i,j) - (\hat{\alpha}(i,j) + \hat{\beta}(i,j)f))^2} \tag{3.18}$$

- **Step 2:** The test statistic is the $Total_{RMSE}$ in (3.18) which measures the amount of the deviation between linear phase response of all sensor pairs and the fitted lines. Figure 3.9. and Figure 3.10. show the distribution of 1000 $Total_{RMSE}$ values of the noise-only and signal plus noise cases for the array of 4 sensors in the short code and long code systems respectively. As shown in figure, it is possible to determine a threshold value, $\gamma_{threshold}$, which decides the presence of a hidden DS-SS signals as,

$$Total_{RMSE} \begin{cases} <\gamma_{threshold} \rightarrow present \\ \geq\gamma_{threshold} \rightarrow not\ present \end{cases}$$

As it is seen $Total_{RMSE}$ is normalized according to the number of frequency points and the number of sensor pairs. The $Total_{RMSE}$ can be modelled as a Gaussian random variable with a specified mean and variance. As shown in Figure 3.9. and Figure 3.10. the mean and the variance of the distribution is maximum in the noise-only case. In the opposite, the mean and the variance is close to zero in the case of high SNR DS-SS signal. $\gamma_{threshold}$ value is specified according to the distribution of the $Total_{RMSE}$ for the noise-only case by checking the standard normal distribution table (Z table) with the required false alarm rate (FAR). Note that the $Total_{RMSE}$ value is based on the phase measurements of the wideband spatial covariance matrix, hence it does not depend on the noise power.

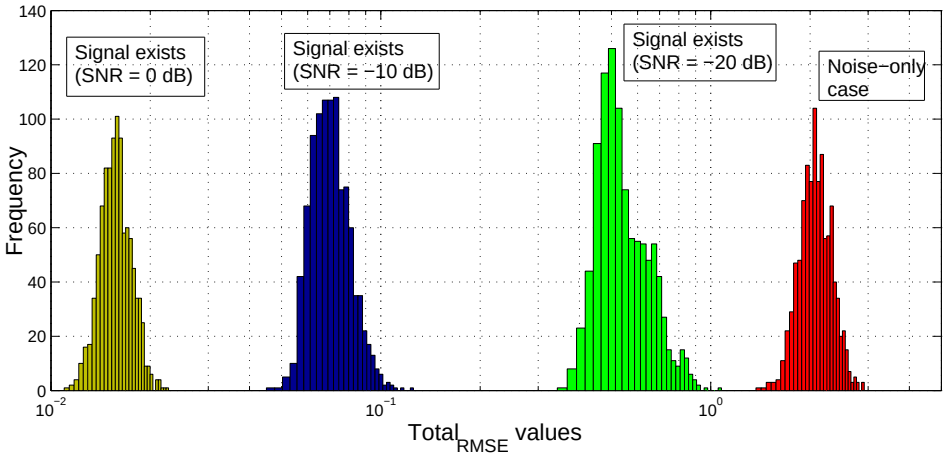

Figure 3.9.: Histograms of the 1000 $Total_{RMSE}$ values for the noise-only case and SNR =-20 dB, -10 dB, 0 dB cases in the short code system.

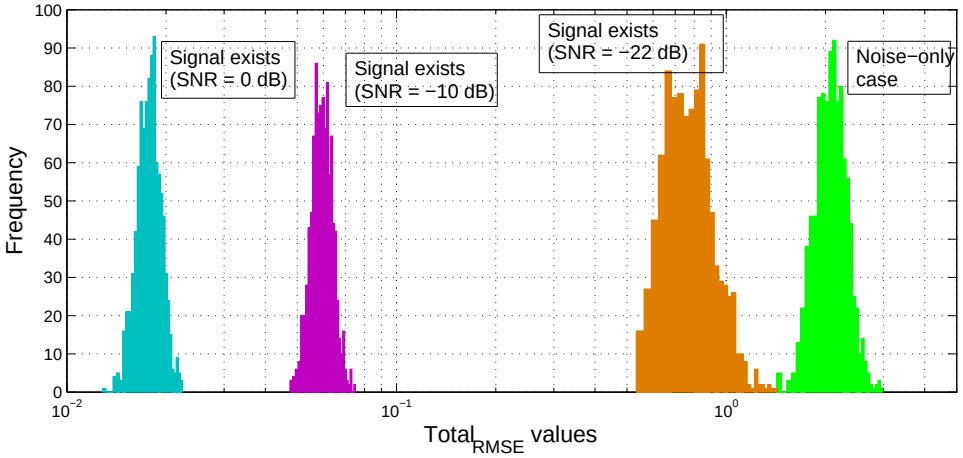

Figure 3.10.: Histograms of the 1000 $Total_{RMSE}$ values for the noise-only case and SNR =-22 dB, -10 dB, 0 dB cases in the long code system.

3.5. Detection of DS-SS Signal Based on Eigenvalue Ratio

In this thesis, a simple and computationally efficient two channel presence detection system is proposed for the noise-like long code DS-SS signals. We first proposed a new method in order to estimate sample spatial covariance matrix for the wideband signal detection in low SNR. Secondly, the presence detection algorithm is proposed which is based on the Eigen Value Ratios (EVR) of the spatial covariance matrices.

In order to process the wideband signals, a common approach is to sample the incoming signals for each channel to form the narrowband frequency components. These narrowband frequency components are processed separately and combined to obtain the final result which is known as incoherent signal-subspace processing (ISSP) method [46]. But the presence detection performance of this approach may be insufficient for the long-code DS-SS signals in low SNR. However, the coherent signal-subspace methods (CSM), which uses focusing matrices to transform the spatial covariance matrices to specific frequency bin, are suitable for solving the wideband signal processing problems with the narrowband methods such as the Akaike information criterion (AIC) and the minimum description length (MDL) algorithms [47]. But the presence detection of the long code DS-SS signals is a pretreatment phase and there is a need for methods which are computationally efficient.

In this thesis, the block of consecutive frequency bins are combined in order to estimate the sample spatial covariance matrices for the presence detection. The relation between the numbers of consecutive frequency bins (in terms of signal bandwidth) and the EVRs of the covariance matrices of the two channel sensor array is shown numerically. As is known, mixing the different frequency component will increase the number of significant eigenvalues which prevents the detection [27]. On the other hand, the covariance matrix estimates which are obtained from the sufficient block of consecutive frequency bins are more stable and suitable for signal detection. In this thesis, a computationally efficient presence detection algorithm is proposed which uses spatial covariance

matrices which are estimated using the block of consecutive frequency bins.

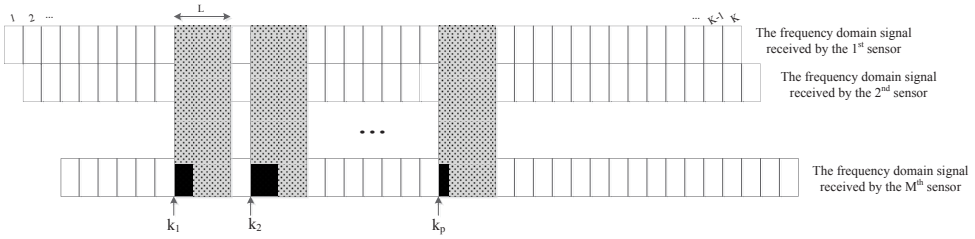

Figure 3.11.: Scheme of the $\mathbf{R}$ matrix estimation using the BCFB method.

A 2×2 spatial covariance matrix in (3.9) and its elements are shown as $\mathbf{R} = \begin{bmatrix} a & b \\ b^* & c \end{bmatrix}$, the eigenvalues ($\lambda_1$ and λ_2) of this matrix can be calculated using its trace ($T = a + c$) and determinant ($D = a \times c - b \times b^*$) as,

$$\lambda_1 = \frac{T}{2} + \sqrt{\frac{T^2}{4} - D}, \qquad \lambda_2 = \frac{T}{2} - \sqrt{\frac{T^2}{4} - D} \tag{3.19}$$

where * stands for conjugate.

In the presence of DS-SS signals, the difference between maximum (λ_1) and minimum (λ_2) eigenvalues increases. The ratio of maximum eigenvalue to minimum one is a decisive parameter. In the presence of signals, this ratio is very high and in the noise-only case since all eigenvalues of $\mathbf{R}$ matrix represent noise subspace, this ratio is close to one. When the frequency bins combined properly, the ratio between maximum and minimum eigenvalues (EigenValue Ratio, $EVR = \lambda_1/\lambda_2$) is determined to be used as an effective test statistics for the presence detection of DS-SS signals.

In order to estimate sample covariance matrices, we proposed a new method which is presented in Section 3.5.2. Firstly, a well-known approach for wideband signal processing, ISSP is overviewed in Section 3.5.1.

3.5.1. Estimating R Matrix Using Incoherent Signal-Subspace Processing (ISSP) Method

In wideband signal processing, the wideband signal is decomposed into narrow bands and the narrowband signals are processed individually. Then the results from each individual bands are combined to obtain the final result [48]. This technique is called as incoherent signal-subspace processing (ISSP). The steps of this approach are summarized below.

- Wideband signal is divided equally into non-overlapping B snapshots.
- The temporal Discrete Fourier Transform (DFT) of the B snapshots is computed and spatial covariance matrices are estimated as below,

$$\hat{\mathbf{R}}_p^{ISSP} = \frac{1}{B}\sum_{b=1}^{B}\mathbf{Y}_{b,p}\mathbf{Y}_{b,p}^H \qquad \begin{matrix} p=1,\ldots,P \\ b=1,\ldots,B \end{matrix} \tag{3.20}$$

where, B is the total number of snapshots and P is the number of frequency bins in each snapshot. $\mathbf{Y}_{b,p}$ represents b^{th} snapshot and the p^{th} frequency component of the sensors output. Furthermore, $\hat{\mathbf{R}}_p$ is an $M \times M$ matrix and there are total P covariance matrices. It is possible to use all the matrices in (3.20) for the presence detection of DS-SS signals using the proposed algorithm in section 3.5.3.

3.5.2. Estimating R Matrix Using The Block of Consecutive Frequency Bins (BCFB) Method

In the practical real time applications, the detection methods using whole components of the received signal are not efficient due to high computational cost. Therefore, transmitting the whole signal from a receiver to another receiver in the multichannel detection system, is very hard. To overcome this difficulty, a new $\mathbf{R}$ matrix estimation method not using the whole signal components is proposed. In this method, some frequency bins are sufficient for the signal detection and the parameter estimation. Firsly, the Discrete Fourier

Transform (DFT) of the outputs at each sensor are computed. The total number of frequency bins (K) are equal to the length of the sensor output data. It is assumed that the baseband signal is in the middle of the band. Then the total F number frequency points ($F < K$) which should be in the bandwidth of spread spectrum signal are chosen symmetrically from the both sides of center frequency of the receivers. Then, the chosen data is divided into non overlapping frequency blocks. But only the some frequency bins in each block will be used. L is the used number of consecutive frequency bins in each block. $\hat{\mathbf{R}}_p$ is the estimated matrix from p^{th} block in sparse structure as the following,

$$\hat{\mathbf{R}}_p^{BCFB} = \frac{1}{L} \sum_{k=k_p}^{k_p+L-1} \mathbf{Y}[k]\mathbf{Y}^H[k] \qquad p = 1, ..., P \tag{3.21}$$

where P is the number of total blocks and k_p is the beginning of p^{th} frequency band. The sparsity is stated in terms of percentage as below,

$$\%Sp = \frac{F - L \times P}{F} \times 100 \tag{3.22}$$

Furthermore, $\hat{\mathbf{R}}_p$ is a matrix of dimension 2×2 and there are total P covariance matrices.

(1) *The selection of L and P parameters*

When estimating a $\mathbf{R}$ matrix, the band of the signal that can be manipulated fully or sparsely, is separated into consecutive frequency blocks. The amount of sparsity is specified respect to the selection of L and P. Ideally, as the whole band is used, there is no gap and no overlap amongst the blocks. In this case, $L \times P$ value covers the signal bandwidth. On the other hand, the number of P can be decreased to avoid high computational complexity which causes sparsely structure.

Besides, the selected P values determine the number of covariance matrices. In order to calculate each spatial covariance matrix in (3.21), L number of frequency bins are used. The selection of L is crucial and directly

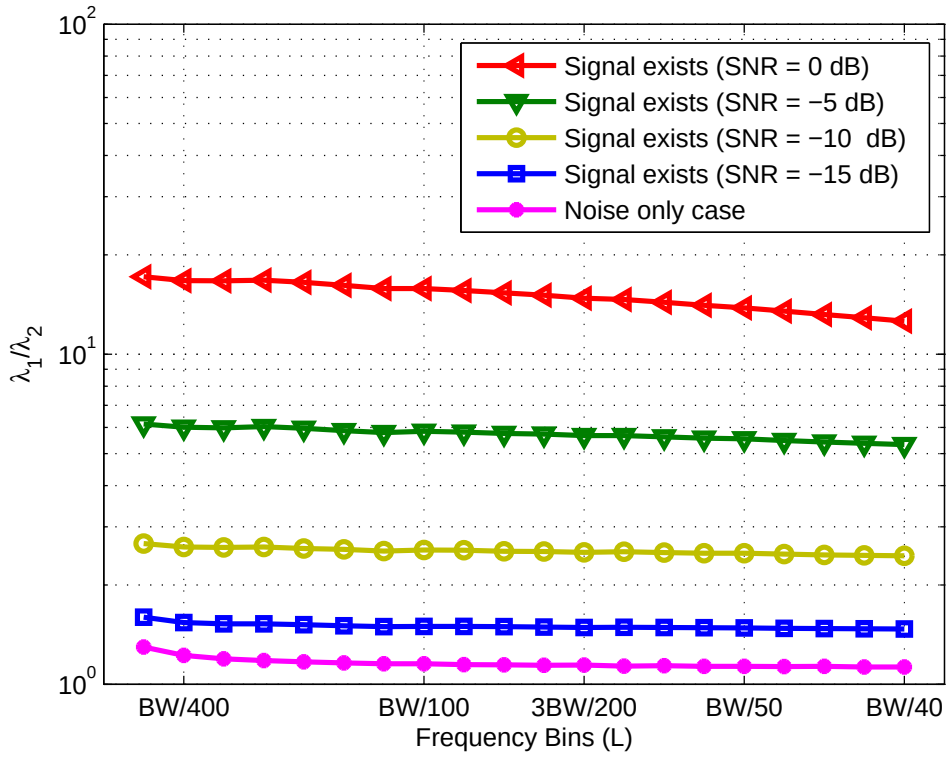

Figure 3.12.: The maximum and minimum eigenvalue ratios (λ_1/λ_2) with respect to L in terms of bandwidth (BW) of the signal.

effects the detection performance of the method. When L is chosen as to cover the whole signal bandwidth, the number of the significant eigenvalues of the $\mathbf{R}$ matrix increases which prevents to distinguish signal and noise subspaces [45]. The maximum and minimum eigenvalue ratios of (3.21) with respect to L (in terms of the signal's bandwidth (BW)) are shown in Figure 3.12. for different SNR levels and for the noise-only case. As it is seen for the noise-only case, increasing L makes this ratio close to one which is desired. On the other hand, when L is chosen bigger than some value ($BW/100$), this ratio is decreasing which is undesired. For these reasons ideally L should be chosen between $BW/200$ and $BW/100$. After specifying L value, the selection of the P value will specify the sparsity level.

3.5.3. Detection Algorithm

- **Step 1:** Calculate $EVRs$ of all the computed P spatial covariance matrices as,

$$EVR_p = \frac{\lambda_1}{\lambda_2} = \frac{1 + \sqrt{1 - \frac{4D_p}{{T_p}^2}}}{1 - \sqrt{1 - \frac{4D_p}{{T_p}^2}}} \tag{3.23}$$

- **Step 2:** The average eigenvalue ratio is calculated by averaging EVR values computed in Step-1 as,

$$EVR = \frac{1}{P} \sum_{p=1}^{P} EVR_p \tag{3.24}$$

- **Step 3:** The EVR value in (3.24) is used as a test statistic in order to detect the DS-SS signals. Figure 3.13. shows the distribution of 1000 EVR values for the noise-only and signal plus noise cases for the array of two sensors. As shown in figure, this ratio is statistically separated each other presence of a DS-SS signal and noise-only case. The threshold value ($\gamma_{threshold}$) is determined according to distribution of EVR in noise-only case and the presence of a signal above this threshold is detected as below,

$$EVR \begin{cases} > \gamma_{threshold} \rightarrow signal\ is\ present, & H_1 \\ \leq \gamma_{threshold} \rightarrow signal\ is\ not\ present, & H_0 \end{cases}$$

The distribution of the EVR values is assumed as a Gaussian distributed random variable with a specified mean and variance as shown in Figure 3.13. for different cases. $\gamma_{threshold}$ value is specified according to the distribution of the EVR for the noise-only case by checking the standard normal distribution table (Z Table) using the required false alarm rate (FAR).

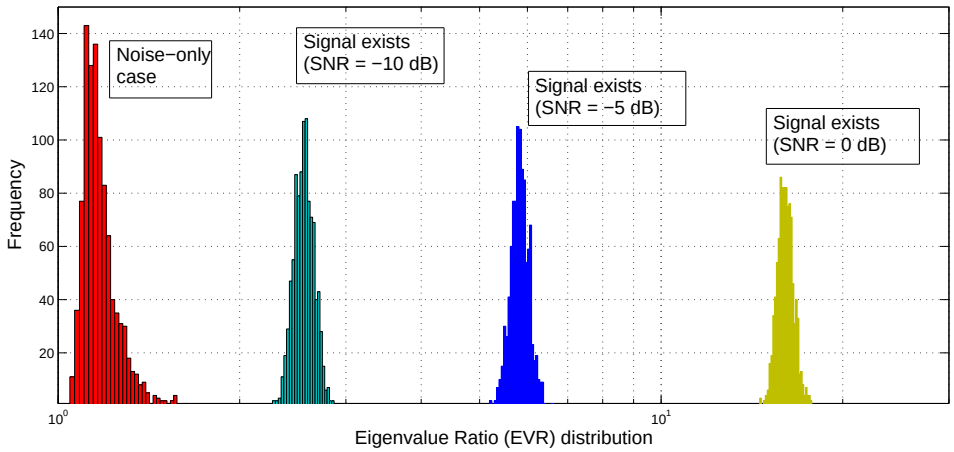

Figure 3.13.: Histograms of the 1000 EVR values for the noise-only case and SNR = 0 dB, -5 dB, -10 dB cases.

3.6. Simulation Results

3.6.1. Simulations for Phase Linearity Based Method

In this section, the proposed non-cooperative multichannel DS-SS signal detection method is evaluated in order to show the detection performance of both the long-and-short code signals for various SNR levels, sensor numbers and spreading sequence length. Besides, the detection performances of the proposed method are given in the presence of narrowband interferences and multipath reflections.

In simulations, the DS-SS signals are generated using the BPSK modulator. Symbol rate is 1000 sym/sec, each symbol is sampled with 8 bits. The sampling rate of the wideband receivers is 100 MHz. The source is located at (8000, 8000). Sensors in the array are positioned linear and equispaced in parallel with the x-axis. The four sensors are located at (0, 0), (100, 0), (200, 0) and (300, 0), respectively. The simulation results are obtained by averaging 1000 Monte Carlo runs. The threshold value, which decides the presence of a DS-SS signal, is selected from the Table 3.1 for the required FAR and the number of sensors.

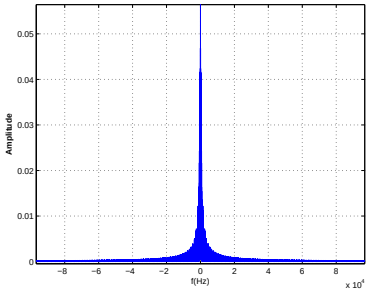

(a) The DFT of the signal before spreading.

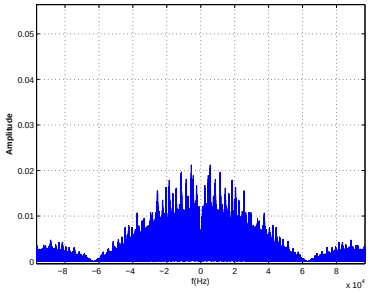

(b) The DFT of the signal after spreading.

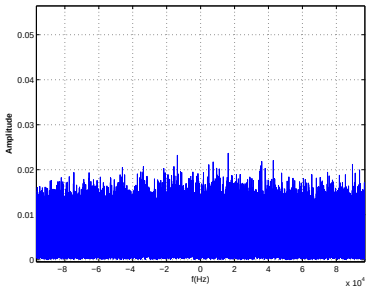

(c) The received noisy signal in the frequency domain.

Figure 3.14.: The different versions of the signal in frequency domain.

The DFT (Discrete Fourier Transform) of the signal before and after spreading are shown in Figure 3.14.a and Figure 3.14.b, respectively. The spreading code is a $2^6 - 1$ bits m-sequence for the signals in the figures. As is seen in the figures, the signal bandwidth expands at the rate of spreading code length. After spreading, the signal is transmitted below the noise level. The received signal in the frequency domain for the SNR=-15 dB case, is shown in Figure 3.14.c. It is seen in the figure, the radiated power of the received signal is below the ambient noise.

a-) **For the short code (SC) DS-SS signals**

Figure 3.15. shows the probability of the short-code (SC) DS-SS signal detection of the proposed method for the different number of sensors (M = 2, 3, 4, 5 and 6) and for the various SNR levels. The length of the PN

Sensor Number (M)	False Alarm Rate (FAR)	$\gamma_{threshold}$
6	0.05	1.86
5	0.05	1.82
4	0.05	1.76
3	0.05	1.58
2	0.05	1.39

Table 3.1: $\gamma_{threshold}$ values for the required FAR and various number of sensors.

sequence is $2^6 - 1$ bits for all performances in this figure. The period of the PN sequence equals the symbol duration (bit period). Even in the array of 2 sensors case, the DS-SS signal can be well detected when the SNR is higher than -20 dB. In this case, increasing the number of sensors improves the detection performance especially in low SNR values as expected. This improvement is more observable up to 5 sensors. However, the cost of the system also increases with the increasing of sensor number. At this point, the main advantage of the proposed method is the ability of detection in quite low SNR levels (below -15 dB). Increasing the number of sensors increases the number of processed sensor pairs. Therefore, the amount of deviation from the linear phase response decreases and the system performs better. The false alarm rate of the proposed method is measured approximately as %5. But this rate can be decreased by adjusting threshold value.

The probability of the short-code (SC) DS-SS signal detection performances of the proposed method for the different length of the PN sequences are shown in Figure 3.16. The proposed method does not require any assumption on the spreading sequence. In cyclostationary based methods, the temporal or spatial duration must be chosen to cover the length of spreading sequence. As the proposed method uses the time delays between the sensors, its detection performance is invariant from the PN sequence length as seen from the figure. In other words, as the proposed method are not based on the cyclic feature of

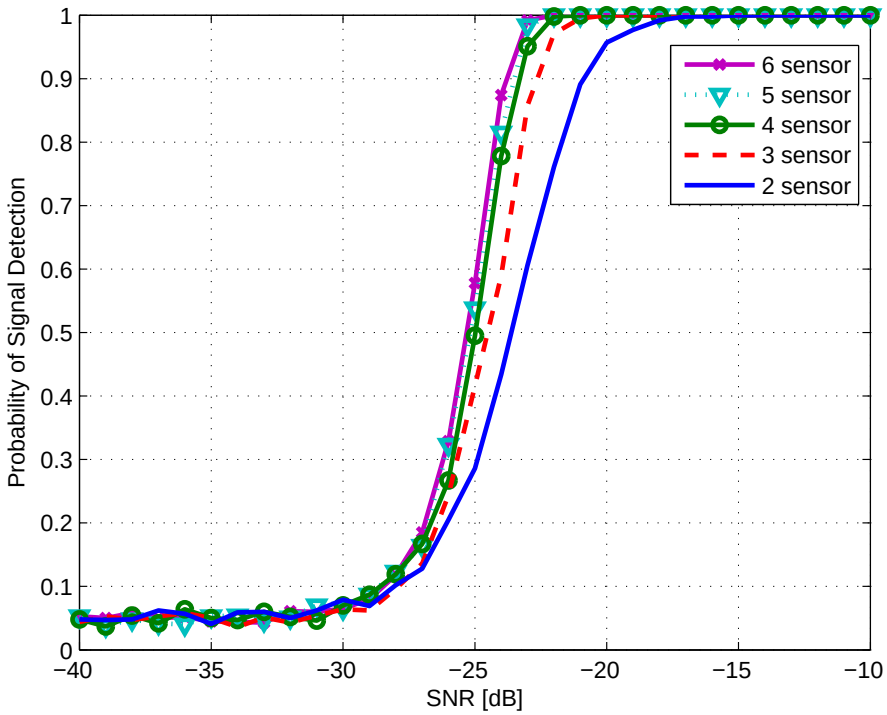

Figure 3.15.: The probability of the SC signal detection of 1000 trials for the array of M = 2, 3, 4, 5 and 6 sensors for various SNR values.

the signal, the length of the spreading code does not matter for the detection performance.

Figure 3.17. demonstrates the performance comparison of the proposed multichannel method and the well-known single channel detection method (Burel's method) [22]. The array of 4 sensors are used for the implementation of the proposed method. The length of the short spreading code is selected as $2^6 - 1$ for both of two methods. In the method of Burel, the length of the temporal window duration which is equally selected as number of frequency bins in one snapshot of the proposed method, is larger than the period of the spreading sequence. When the detection performances are compared, it is seen that the proposed method performs better than the method of Burel. It is seen in the figure, the proposed method improves the detection performance about 12 dB according to the Burel. As Burel uses the cyclostationary properties of

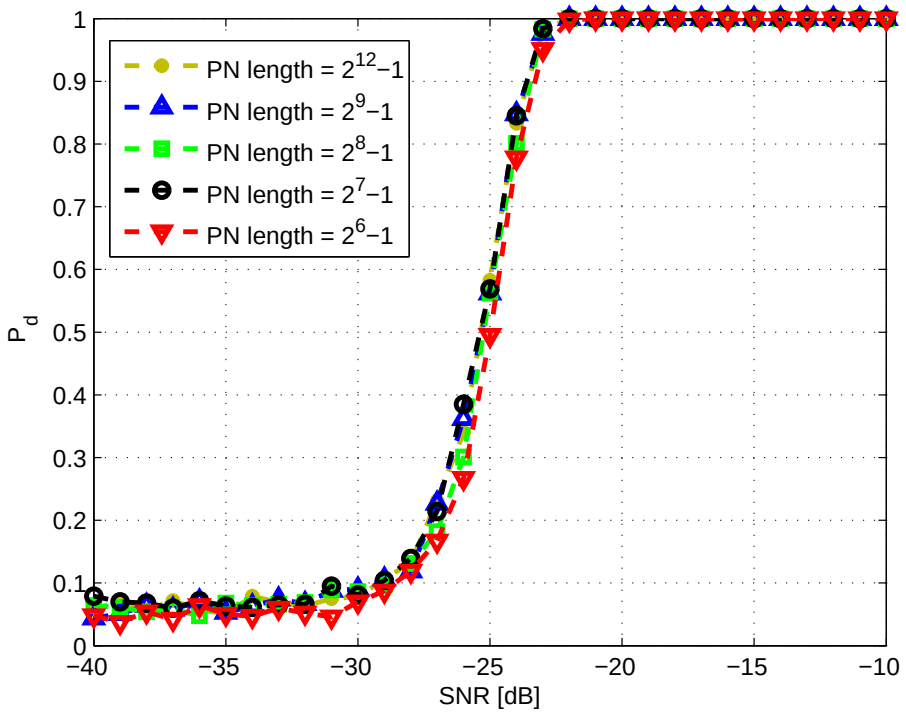

Figure 3.16.: The probability of the SC signal detection of 1000 trials for array of 4 sensors for the different PN sequence lengths.

the signal, the temporal window duration used in his method should be larger than the length of the PN sequence. The detection performance of the Burel's method is badly affected with the increasing of the PN sequence length, on the other hand our proposed method is invariant from the PN sequence length as mentioned previously. When the PN sequence length increases, the window can not cover a spreading code period. Thus, the detection performance worsens.

Figure 3.18. shows the detection performances of the proposed method in the presence of multipath fading and narrowband interference. In simulations, a stationary multipath scenario where the signal is received through two distinct paths, is realized. The path delays and gains are chosen same with the delays in [20]. It is shown in figure, in multipath case, the detection performance of the proposed method is not effected in SNRs higher than

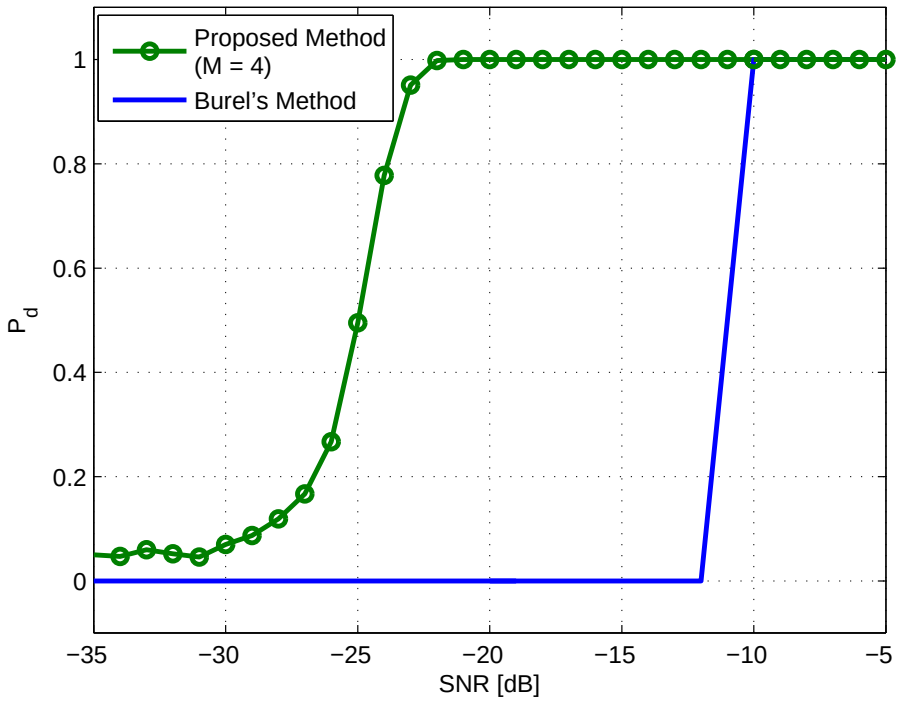

Figure 3.17.: The comparison of the SC detection performances between the proposed method and Burel's method for same PN sequence length.

-20 dB. However, a slight performance loss is experienced below -20 dB. It is understood that the proposed method does not require line of sight conditions between the transmitter and each receivers. Better performance will be achieved with the increasing the number of sensors. In addition, Figure 3.18. also shows the detection performance of the proposed method in the presence of narrow band interference and both the narrow band and multipath signals. It is seen that the proposed method is resistive to these effects.

b-) **For the long code (LC) DS-SS signals**

The LC signal detection performances of the proposed method according to the different number of sensors (M = 2, 3, 4, 5 and 6) for the various SNR levels are shown in Figure 3.19. The length of the PN sequence is selected $2^{12} - 1$, the spreading factor is selected 455 for the signals in this graphics. Unlike the SC DS-SS systems, the spreading factor is less than the

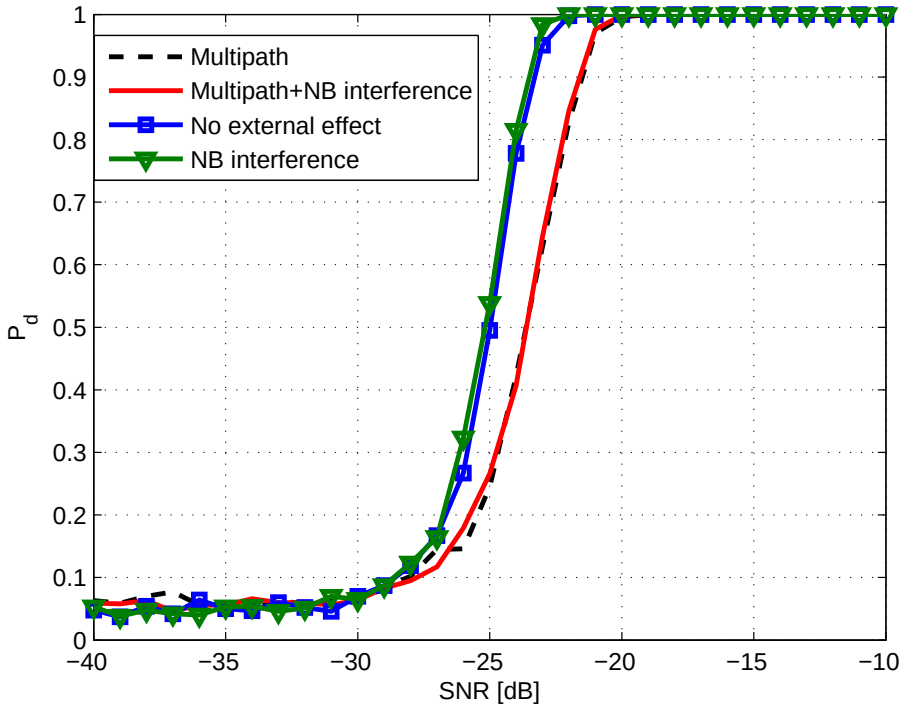

Figure 3.18.: The probability of the SC signal detection of 1000 trials for array of 4 sensors when the multipath and narrow band interference are present.

length of the spreading sequence. It is seen that the detection performances are similar with the results for the SC DS-SS signals. Increasing the number of sensors also enables to detect DS-SS signals in lower SNR levels. But the detection performance does not improve dramatically with the increasing of the sensor number after 4 sensors. As mentioned previously, long spreading codes destroys the cyclostationary properties of the signal. Thus, the methods which use cyclostationary properties of the signal do not work with LC DS-SS signals. To our knowledge, there is no multichannel detection method that uses the phase linearity for long-code DS-SS signals in literature.

The long-code signal detection performances of the proposed method under multipath environments and narrowband interference are shown in Figure 3.20. In multipath environments, in addition to direct-path signal, the delayed and attenuated versions of the target signal is received by each sensor.

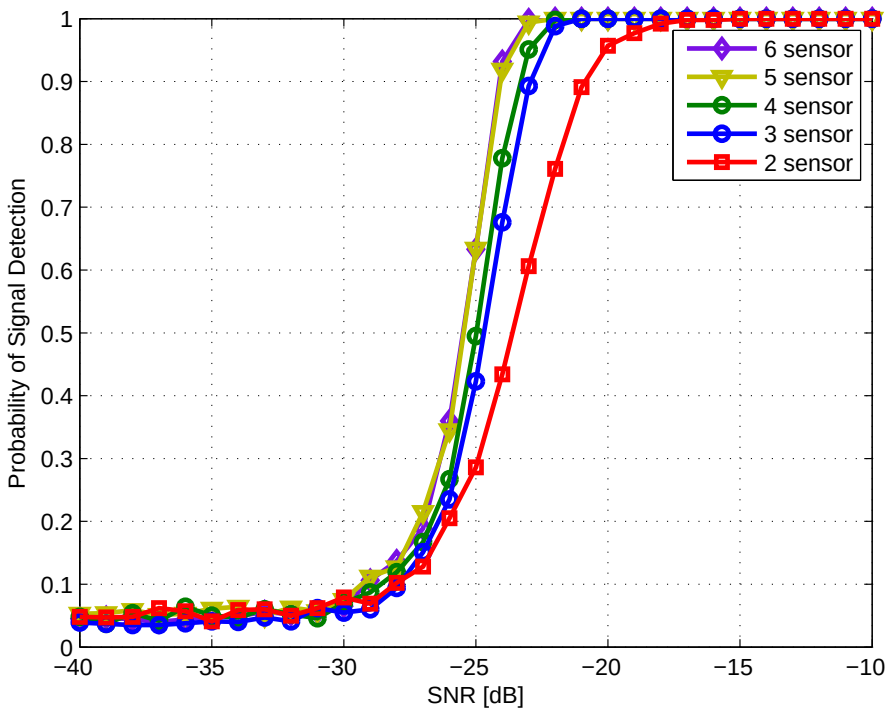

Figure 3.19.: The probability of the LC signal detection of 1000 trials for the array of M = 2, 3, 4, 5 and 6 sensors for various SNR values.

It is dealt that the transmitted signal is reflected from the stationary reflector located at (2000, 2000). The multipath parameters (path delay and gain) are chosen same as the short-code cases. It is shown in figure the long-code signal detection performance of the proposed method is not effected significantly in multipath case. The usage of multiple sensors provide redundancy for the signal detection under multipath environments. In addition, it is seen in the figure, there is no performance degradation depends on the presence of a narrowband interferer. It is understood that the proposed method is resistive to these effects as well as the short-code case.

The cyclostationary-based algorithms cannot be used with long code signals. The reason of this is referred in the previous sections. Thus, Burel's method in [22] which uses cyclic features of the signal does not work with LC DS-SS signals. Hence, the only short code detection performance is compared

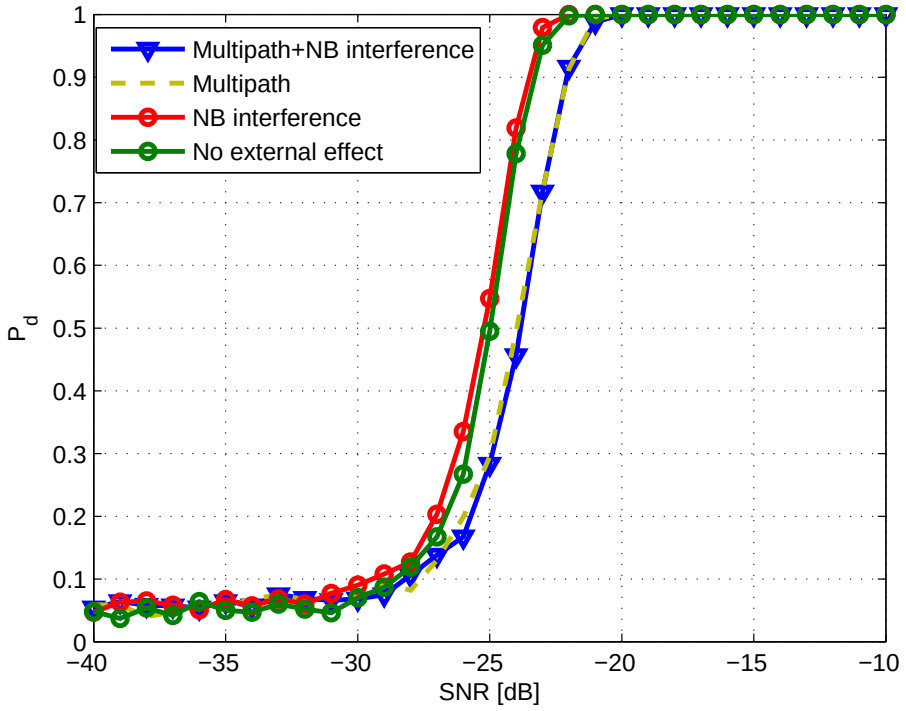

Figure 3.20.: The probability of the long-code signal detection of 1000 trials for array of 4 sensors when the multipath and narrow band interference are present.

with the Burel's method.

3.6.2. Simulations for Eigenvalue Ratio Based Method

In this part, the proposed eigenvalue ratio based method is tested through simulations by using two-channel DS-SS detection system. The simulation results are obtained by averaging 1000 Monte-Carlo runs.

In simulations, the DS-SS signals are generated using the BPSK modulator. The length of the long spreading sequence is $2^{12} - 1$ bits. Symbol rate is 1000 sym/sec. The threshold value which decides the presence of a DS-SS signal is calculated as 1.36 by using standard normal distribution table for the FAR=0.05.

In order to estimate sample covariance matrices, we used two methods. The first method is the ISSP method. The number of blocks in (3.20) is selected

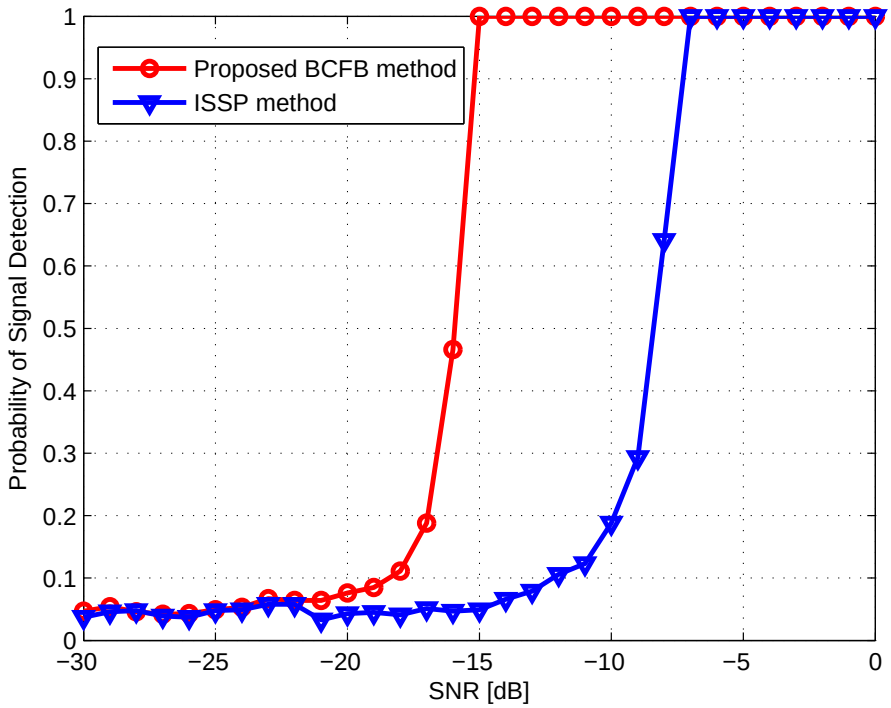

Figure 3.21.: Comparison of detection performances between the proposed method based on BCFB and ISSP for array of two sensors for different SNR values.

as $B = 640$ and each block has 500 samples. The number of DFT points in each block is 200. The second one is the proposed BCFB method and the parameters in (3.21) are selected as $P = 3$ and $L = BW/200$.

Figure 3.21. shows the effect of the $\mathbf{R}$ estimation to the detection performance of the proposed methods. It is seen in the figure that using $\mathbf{R}$ matrices of the proposed method BCFB method improves the detection performance about 8 dB. The BCFB method gives stable $\mathbf{R}$ estimates especially in low SNR. At this point, the main advantage of the proposed method is the ability of detection in quite low SNR levels (below -10 dB). When SNR is below -8 dB, the performance of ISSP dramatically decreases as expected since that is an incoherent method.

Figure 3.22. shows the ROC curves (P_d vs. P_{fa}) for some low SNR values (-20 dB, -18 dB, -17 dB, -16 dB and -14 dB). The probability of signal detection takes different values according to different FAR (threshold) values.

As seen in ROC curves, the probability of signal detection of the proposed method reaches 1 at $P_{fa} = 0.03$ when SNR=-16 dB. It is understood from the figure, when the FAR changes, which values the probability of signal detection will take, is determined according to the different SNR levels.

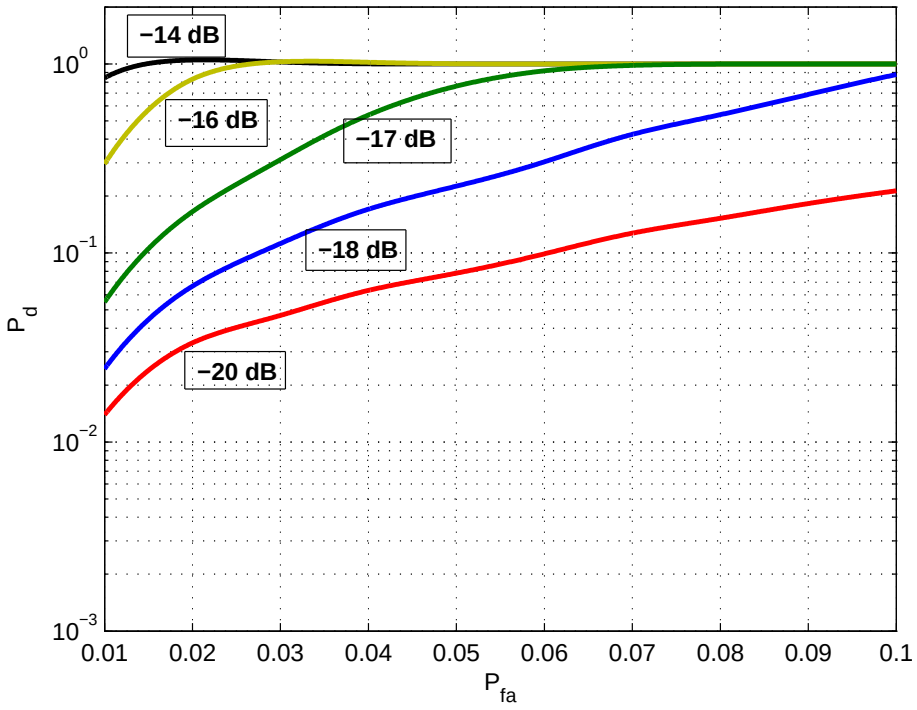

Figure 3.22.: ROC curves (Probability of signal detection (P_d) - probability of false alarm (P_{fa})) in different SNR for array of two sensors.

The detection performance of the proposed method in multipath case for various sensor number is shown in Figure 3.23. The signal is transmitted through two distinct path in a stationary multipath scenario. The path delays and gains are chosen as same with the values in [20]. As seen from the figure, the detection performance of the system decreases in the presence of multipath reflections. It is also seen that increasing the number of sensors improves the detection performance as expected. Furthermore, the proposed method can be implemented for M channel sensor arrays.

The execution times comparison between the proposed eigenanalysis based detection method and the proposed phase linearity based detection

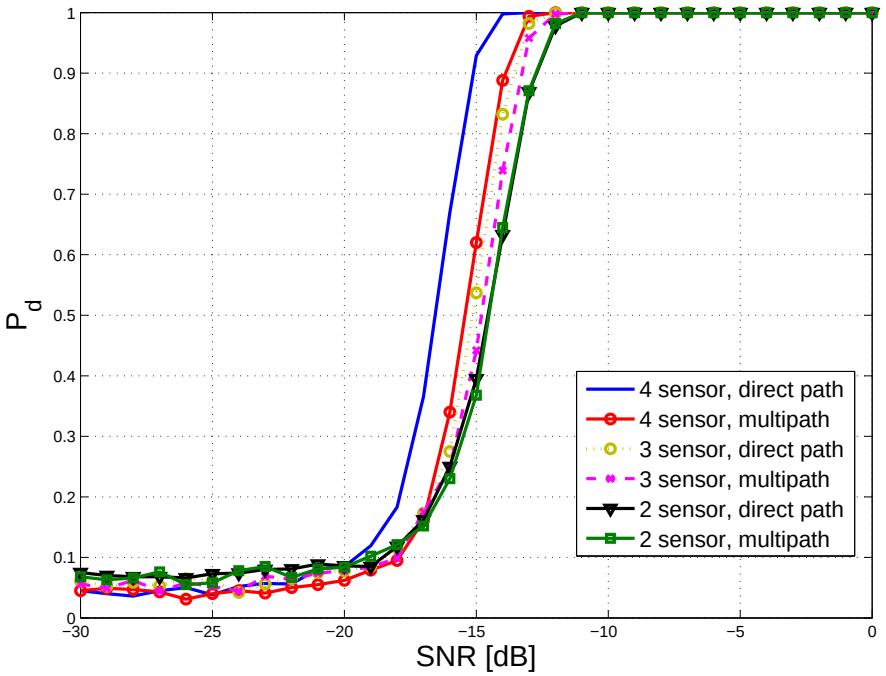

Figure 3.23.: The direct path-multipath performances of the proposed method for the array of $M = 2$, 3 and 4 sensors.

method are given in Table 3.2. Only the short-code signals are tackled for the computation. The values in the table are the total execution durations of the 1000 runs. The simulations run on the computer which has Intel Core(TM) i7-3770K CPU @ 4.60 GHz Processor and 16 GB RAM. The execution times may vary depend on the features of the computer. The eigenvalue ratio algorithm is an applicable technique in practical real time applications due to its simple and fast structure. It is seen in Table 3.2 that the second proposed method is 26 times faster than the first proposed method for the array of 2 sensors. While the detection performance of the first proposed method is better than the second proposed method, the computational cost of the second one is much lower than the first one.

	Method I (Phase Linearity)	Method II (Eigenvalue Ratio)
2 Sensor	690 sec	25.90 sec
3 Sensor	716 sec	40.31 sec
4 Sensor	750 sec	55 sec

Table 3.2: The total execution times for the Phase Linearity and Eigenvalue Ratio algorithms as a result of 1000 trial.

3.7. Conclusion

In this thesis, two different multichannel methods are proposed for the presence detection of both the long and short code DS-SS signals. The proposed methods can detect the DS-SS signals in a stable way in low SNR without any prior information and assumption on target signal. The first proposed method uses the phase linearity of the cross channel terms of the spatial covariance matrices along to the signal bandwidth. It is shown in simulations that the proposed multichannel method can decidedly detect the DS-SS signals in low SNR. It is seen, increasing the number of sensors improves the detection performance as expected. The proposed method can also effectively detect the short-code DS-SS signals which outperforms Burel's method in [22]. In the method of Burel, the temporal window length should be chosen approximately in order to detect the SC DS-SS signals. Finally, it is shown in simulations that the proposed method is resistive to narrowband interferences and multipath fading.

In the second proposed method, we proposed a statistical signal detection algorithm using average of eigenvalue ratios of the spatial covariance matrices ($\mathbf{R}$) of the wideband signal. In addition, a new sample spatial covariance matrix ($\mathbf{R}$) estimation technique, which is called as block of consecutive frequency bins (BCFB), is proposed. The BCFB method gives a stable $\mathbf{R}$ estimate especially in low SNR. Also the proposed BCFB method is not using the whole frequency components of the signal. It is shown in various simulations

that the proposed detection methods can detect DS-SS signals in a stable way in low SNR. It is also shown that using the sample covariance matrix of the proposed BCFB method improves the detection performance especially in low SNR. In the presence of multipath reflections, it is seen that increasing the number of sensors improves the detection performance.

4. TDOA ESTIMATION OF SPREAD SPECTRUM SIGNALS

4.1. Introduction

Source localization is an important problem in applications such as target tracking, surveillance, navigation, and others. Generally, target signals can be localized by using the time of arrival (TOA), the time difference of arrival (TDOA), the angle of arrival (AOA), the received signal strength (RSS) and Doppler frequency shift measurements [49–51].

Time delay estimation is still an active research field and there are some important applications in many areas such as radar, sonar and wireless communication systems for localizing and tracking targets. If we have a priori knowledge for the transmitted signal, it is possible to estimate time delays. On the other hand, in the case of unknown transmitted signal, only the time difference of arrival (TDOA),τ, between the spatially distributed sensors can be estimated. Here, one of the sensors should be defined as the reference sensor. The time difference,τ, between the reference sensor and the m^{th} sensor is defined as,

$$\tau = \frac{d_m - d_r}{c} \tag{4.1}$$

where, d_m and d_r are the distances from the source to m^{th} sensor and to the reference sensor, respectively. c is the propagation speed. A simple TDOA illustration is shown in Figure 4.1., here one source is assumed to be in the far field and two sensors are utilized. TDOA measurements can be used to localize a radio [52], sonar [53] or acoustic emitting sources [54–57]. TDOA-based localization is widely studied in literature. These methods can be classified in pairs as the following: Likelihood based method and least square technique, linear approximation and direct numerical optimization (maximization and minimization), and iterative and closed form algorithms [58]. Some of these studies have been concentrate on the TDOA-based maximum likelihood (ML)

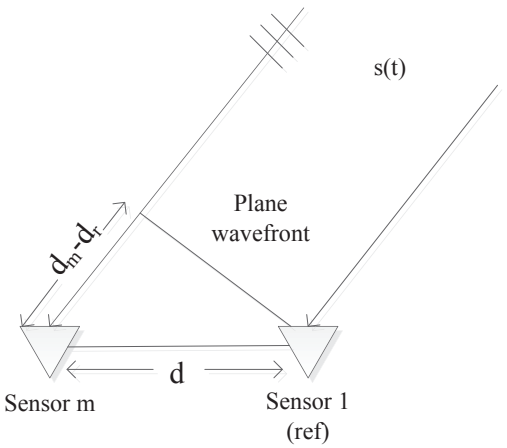

Figure 4.1.: The TDOA illustration

localization [59–61]. Generally, the ML approaches need an initial guess and iterative solutions to converge the optimal solution, and also convergence cannot be guaranteed. Hence, in the real-time applications of a source localization, ML estimators are not convenient [58]. To overcome this disadvantages, the closed-form solutions have been developed [62–65]. Closed-form algorithms utilize the least square technique which is the other common approach for TDOA-based localization. Linear least square technique is widely preferred because of its computational efficiency. In [63], a closed-form localization technique which is called spherical-interpolation (SI) method, is proposed. In the SI method, linear least squares minimization is used for the derivation of the localization formulas. In [58], the linear-correction least-squares approach have been proposed for the source localization problem. This method use the additive measurement error model, and this model assumes that additive errors are independent from the measurements. This least square estimator has a closed-form algorithm and it is suitable for the real-time applications. In [66], an importance sampling method is proposed in order to determine a global solution to the ML source localization problem. But this method requires an initial estimate for the source location.

In order to estimate TDOA, there are various methods which are based on cross-correlation technique [67], phase data [44, 68–71], least squares [68–70] and maximum likelihood [69, 72]. Well-known time difference of arrival estimation techniques are based on cross correlation of the received signals at different sensors. The peak of the cross correlation output gives the time difference of arrival between the sensors. Cross correlation based methods can be implemented easily and they are simple methods as well. For this reason, they are widely used in the estimation systems. On the other hand, this techniques are not effective in the presence of multipath reflections. In [73], a TDOA estimator for acoustic signals which uses a multichannel spatio-temporal prediction algorithm is presented. This method uses both the spatial and temporal information in minimum mean square error sense. In [71], a time delay estimator using the phase differences between two sensors is proposed. The main idea in this method is averaging the phase differences in the pass band frequency. In [68], a least squares algorithm is developed to estimate TDOA in multipath environments. The algorithm in this method gives least squares estimates of the time delay of each signal path. In [72], a maximum likelihood (ML) time delay estimator which uses a non-iterative approach is developed. They proposed a importance sampling technique to find the global maximum of the likelihood function. As this method uses the importance sampling method, it does not require grid search and any initial guess unlike the conventional ML techniques.

In this thesis, an efficient frequency domain time difference of arrival estimation method for the spread spectrum signals is proposed. The proposed TDOA estimator uses the phase slope of the previously estimated sample covariance ($\mathbf{R}$) matrices in the first proposed detection method. The phase values of the all $\mathbf{R}$ matrices are estimated with the well-known Root-MUSIC algorithm. Thus, the phase response is obtained with combining all the estimated phase values. After phase unwrapping which is the process that corrects phase angles to produce smoother phase plots, a line is fitted to unwrapped phase response along the signal bandwidth in least square senses. Then TDOA is

estimated by using the slope of the fitted lines.

4.2. Data Model

In this section, the used data model is given. The DS-SS signal is received by two widely separated sensors.

Non-cooperative two channel DS-SS system collects the wideband signals. These sensors are located at known positions $[x_i, y_i]$, $i = 1, 2$. If the sensors (wideband receivers) are coherent and synchronously sampled, the baseband output of i^{th} sensor is,

$$y_i[n] = s[n - \Delta_i] + w_i[n], \qquad n = 1, ..., N \tag{4.2}$$

where $s[n]$ is the transmitted signal, i is sensor index, Δ_i is time shift between i^{th} sensor and reference sensor. N is the number of samples collected from each receiver. The i^{th} sensor output in frequency domain is given as,

$$Y_i[k] = e^{-j2\pi k\Delta_i/K} S[k] + W_i[k], \qquad k = 1, ..., K \tag{4.3}$$

where k is the index of the frequency bins, K is the total number of frequency points. The sensor output vector of 2 sensors in frequency domain is given as,

$$\mathbf{Y}[k] = \mathbf{A}[k]S[k] + \mathbf{W}[k], \qquad k = 1, ..., K \tag{4.4}$$

The wideband spatial covariance matrix of k^{th} frequency bin is defined as,

$$\mathbf{R}[k] = E\{\mathbf{Y}[k]\mathbf{Y}^H[k]\} \tag{4.5}$$

$$\mathbf{R}[k] = \mathbf{A}[k]R_s[k]\mathbf{A}^H[k] + \sigma^2\mathbf{I}[k] \tag{4.6}$$

where $(.)^H$ denotes the conjugate transpose of a matrix. It is assumed that the

noise, **W** is temporally and spatially uncorrelated, white, zero mean Gaussian and has σ^2 variance. **A** is the manifold matrix and **I** is the identity matrix. It is assumed that, there is a single wideband signal, $S[k]$, and the signal covariance is,

$$R_s[k] = E\{S[k]S^H[k]\} \tag{4.7}$$

4.3. Time Difference of Arrival Estimation Based on the R Matrix

In previous chapter, two different multichannel presence detection methods for the DS-SS signals are proposed and discussed. In this part, a new TDOA estimation method uses the phase linearities similar to detection methods for the localization of the DS-SS signals.

4.3.1. Estimating the Sample R Matrices

In order to estimate wideband sample covariance matrix, **R**, we used two methods. The first technique is a well-known Incoherent Signal Subspace Processing (ISSP) method which is given in Section 3.5.1. In this technique, the wideband signal is divided into equally narrow bands and the narrow band data are processed individually. Subsequently, the results from each band are combined to obtain the final result [48]. The sample covariance matrices are estimated as below,

$$\hat{\mathbf{R}}_p^{ISSP} = \frac{1}{B}\sum_{b=1}^{B} \mathbf{Y}_{b,p}\mathbf{Y}_{b,p}^H \qquad \begin{matrix} p=1,\ldots,P \\ b=1,\ldots,B \end{matrix} \tag{4.8}$$

where, B is the total number of snapshots and P is the number of frequency bins in each snapshot. $Y_{b,p}$ represents b^{th} snapshot and the p^{th} frequency component of the sensors output. Furthermore, $\hat{\mathbf{R}}_p$ is an $M \times M$ matrix and there are P covariance matrices.

We proposed a new wideband sample covariance matrix, **R**, estimation method [38]. The proposed method, which is called as block of consecutive

frequency bins (BCFB), uses a sparse estimation. In this method, firstly, the Discrete Fourier Transform (DFT) of the output at each sensors are computed. The total number of frequency bins (K) are equal to the length of the sensor output data. It is assumed that the baseband signal is in the middle of the band. Then the total F number frequency points ($F < K$) which should be in the bandwidth of spread spectrum signal are chosen symmetrically from the both sides of center frequency of the receivers. Then, the chosen data is divided into non overlapping frequency blocks. But only the some frequency bins in each block will be used. L is the used number of frequency points of the blocks. $\hat{\mathbf{R}}_p$ is the estimated matrix from p^{th} block in sparse structure as the following,

$$\hat{\mathbf{R}}_p^{BCFB} = \frac{1}{L} \sum_{k=k_p}^{k_p+L-1} \mathbf{Y}[k]\mathbf{Y}^H[k] \qquad p = 1, ..., P \tag{4.9}$$

where P is the number of total blocks and k_p is the beginning of p^{th} frequency band. The sparsity is stated in terms of percentage as below,

$$\%Sp = \frac{F - L \times P}{F} \times 100 \tag{4.10}$$

Furthermore, $\hat{\mathbf{R}}_p$ is an 2×2 matrix and there are total P covariance matrices. In both approaches, the total P sample covariance matrix, $\hat{\mathbf{R}}_p$ is estimated and the phase values of each matrix is estimated with well-known Root-MUSIC algorithm. It is also straightforward to expand this approach to M channel case.

4.3.2. Phase Estimation with the Root-MUSIC Algorithm

The Root MUSIC is the root version of the well-known MUSIC (Multiple Signal Classification) algorithm [74]. In order to estimate the phase content of the signal, the Root MUSIC algorithm performs eigenvector analysis of the sample covariance matrix of the signal [75]. This algorithm is very useful for

the signals embedded in additive white Gaussian noise. The main idea of the Root MUSIC algorithm is to find the roots of the polynomial of order $2(M-1)$, where M is the number of sensors [76]. This method is only applicable to linearly shaped sensor arrays.

For a linear array, the array manifold vector is given as,

$$\boldsymbol{v}_z(z) = [1 \; z \; ... \; z^{N-1}]^T, \tag{4.11}$$

the array manifold vector in terms of phase shift is shown as,

$$[\boldsymbol{v}_z(z)]_{z=e^{j\phi}} = e^{j(\frac{N-1}{2})\phi}\boldsymbol{v}(\phi). \tag{4.12}$$

The MUSIC algorithm is defined in [77] as,

$$\hat{Q}_{MU,z}(z) = \boldsymbol{v}_z^T(\frac{1}{z})\hat{\boldsymbol{U}}_N\hat{\boldsymbol{U}}_N^H\boldsymbol{v}_z(z) \tag{4.13}$$

here, $\hat{\boldsymbol{U}}_{\boldsymbol{N}}$ represents eigenvectors of the noise subspace. Then (4.13) can be written as,

$$\hat{Q}_{MU,z}(z)|_{z=e^{jw}} = \hat{Q}_{MU}(\phi). \tag{4.14}$$

Then, number of D roots of $\hat{Q}_{MU}(\phi)$ are computed that corresponds D source signals. These roots are given as,

$$\hat{\phi}_i = arg \; \hat{z}_i, \qquad i = 1, 2, ..., D \tag{4.15}$$

As a summary, the steps of the Root MUSIC algorithm are given in the following,

- Estimate the sample covariance matrices according to (4.8) or (4.9).
- Compute the eigenvectors corresponding signal and noise subspaces.
- Compute the roots of $\hat{Q}_{MU}(\phi)$ in (4.14).
- Find the phase as in (4.15).

4.3.3. Phase Unwrapping and Line Fitting

After the phase estimation, the obtained phase responses (total P phase values) are unwrapped for the smooth slope calculation. Phase unwrapping (PU) is the process of recovering the absolute phase ϕ from the wrapped phase ψ [78].

$$\phi = \psi + 2k\pi \tag{4.16}$$

where ϕ and ψ are the true phase value and the wrapped (modulo-2π) phase value, respectively. k is an integer for the number of 2π multiples. After unwrapping, a straight line is fitted to the phase response throughout Z points by using a linear model which is defined as,

$$\phi_z = \alpha + \beta z, \quad z = \frac{P-Z}{2} + 1, ..., \frac{P+Z}{2} \tag{4.17}$$

where z is the frequency bin index, α is an initial point and β is slope of the fitted line. P is the number of phase values in the phase response. The Z points ($Z < P$) which should be in the mid-part of the phase response are chosen symmetrically from the both sides of center point of the phase response. The model in (4.8) can be expressed as,

$$\mathbf{v} = \mathbf{H}\boldsymbol{\theta} + \mathbf{w} \tag{4.18}$$

where $\mathbf{v}$ is the observed data set and $\mathbf{w}$ is the unknown noise which represents the deviation from the model. $\mathbf{H}$ is the known observation matrix,

$$\mathbf{H} = \begin{bmatrix} 1 & \frac{P-Z}{2} + 1 \\ \vdots & \vdots \\ 1 & \frac{P+Z}{2} \end{bmatrix}_{\mathbf{Z}\times\mathbf{2}} \tag{4.19}$$

and finally $\boldsymbol{\theta}$ is the unknown parameter vector $\boldsymbol{\theta} = [\alpha\ \beta]^T$. Hence, the parameters of the fitted lines can be estimated as,

$$\hat{\boldsymbol{\theta}} = (\mathbf{H^T H})^{-1}\mathbf{H^T v} \tag{4.20}$$

which is the minimum variance unbiased estimator for the given model in (4.18). Thus, the estimated coefficients in (4.20) are the optimum line parameters of $\hat{\phi}_z = \hat{\alpha} + \hat{\beta} z$.

In some cases especially in low SNR, the phase is not unwrapped correctly. Accordingly, this situation causes that the slope of the fitted line is estimated incorrect. An unwrapped phase response and a line fitted to

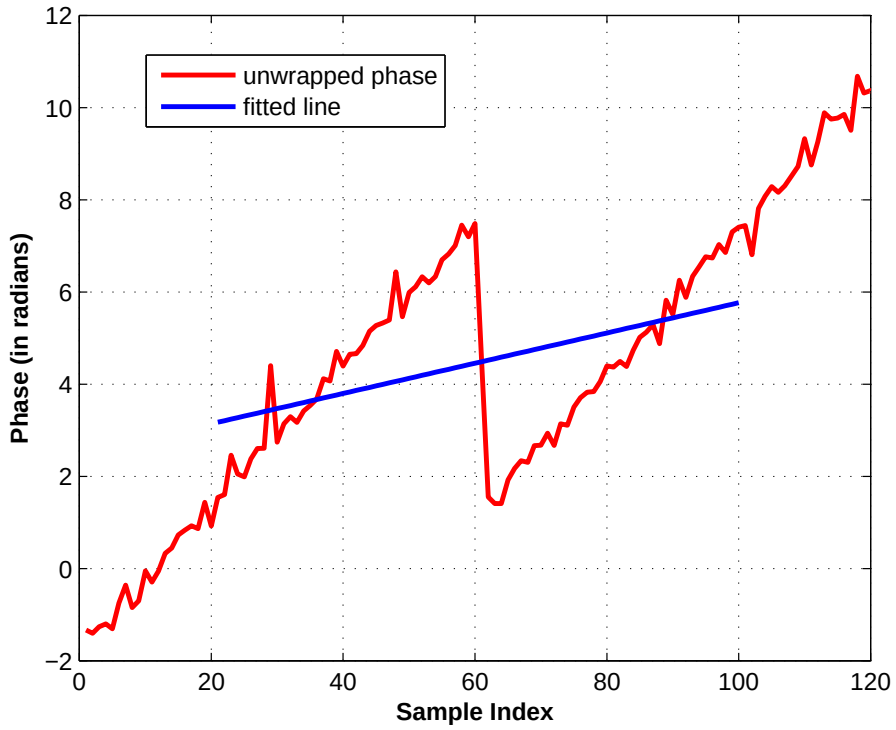

Figure 4.2.: An unwrapped phase and a fitted line to this phase.

this phase are shown in Figure 4.2. In this case, the estimated TDOA value is quite different from the actual value. Therefore, the error between the

real and the estimated value will be very high. To overcome this situation, phase unwrapping algorithm is improved. In the well-known phase unwrapping algorithm, it is tackled whether the difference between the consecutive phase values bigger or smaller than $\pm\pi$. In the improved algorithm, the sum of the differences between the consecutive two phase pair is considered. Thus, the incorrect unwrapping in the phase response are inhibited and the error rate decreases. This case are shown in Figure 4.3.

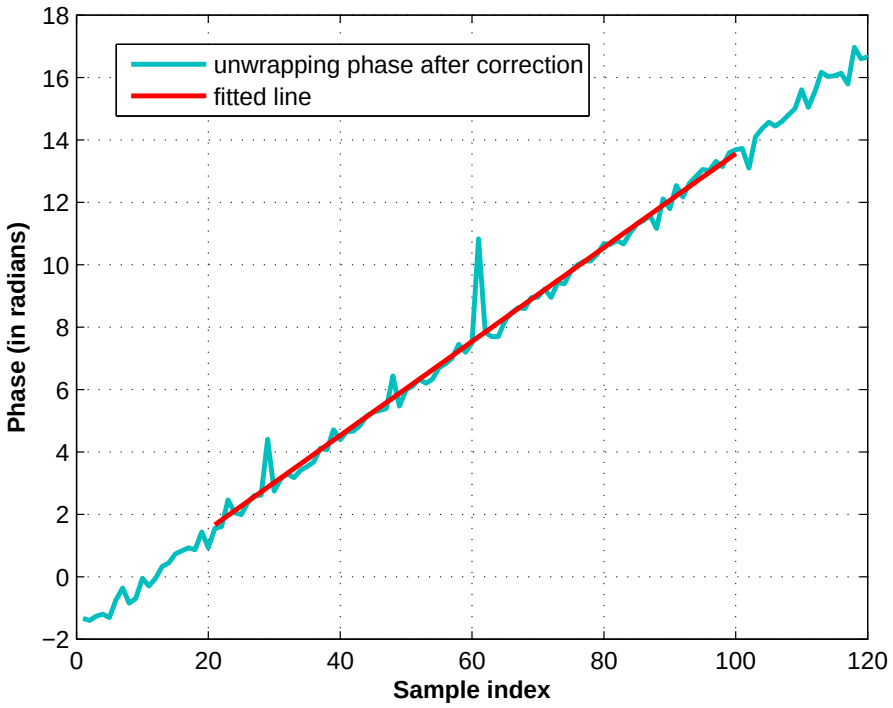

Figure 4.3.: An unwrapped phase after error correction and a fitted line to this phase.

4.3.4. Slope Calculation

As in the first proposed detection method, to estimate TDOA, in this method,

- The sample covariance ($\mathbf{R}$) matrices are estimated.
- The phase of the cross channel terms of $\mathbf{R}$ is computed and the phase response is obtained.

- A straight line is fitted to the phase response.

- The slope of this fitted line is estimated.

And using this slope, TDOA is calculated. The phase value of the one of the cross channel terms of the **R** matrix equals,

$$\phi_k = \frac{2\pi k \Delta}{K} \tag{4.21}$$

where k is the frequency bin index and K is the number of total frequency bins. According to the K frequency bins, the equation of the fitted line is defined as $\hat{\phi_k} = \hat{\beta} \times k$. Then time delay is obtained as following,

$$\hat{\Delta} = \frac{\hat{\beta} \times K}{2\pi} \tag{4.22}$$

As the **R** matrices are estimated using the ISSP method, the phase response is plotted with P points. Accordingly, the slope of the fitted line changes according to the P points. Then the new slope equals $\beta' = \beta \times \frac{P}{K}$. In this case, TDOA is estimated as following,

$$\hat{\Delta}' = \frac{\hat{\beta} \times P}{2\pi} \tag{4.23}$$

The slope of the fitted lines changes according to amount of the used frequency bins. When the **R** matrices are estimated using the BCFB method, a phase value represents F/P frequency bins. Consequently, the slope changes with this ratio, $\beta' = \beta \times \frac{P}{F}$. In this case, TDOA is estimated as below,

$$\hat{\Delta}' = \frac{\hat{\beta} \times K}{\frac{F}{P} \times 2\pi} \tag{4.24}$$

4.3.5. Cramer-Rao Lower Bound on TDOA Estimation

In the estimation problems, the Cramer-Rao lower bound (CRLB) which is a well-known term, is used as a lower bound for the error variance of unbiased estimators. A comprehensive derivation of the CRLB for TDOA estimation is given in [79, 80]. The CRLB is defined for a time continuous model as the following,

$$CRLB(\Delta_t) = \frac{3}{16\pi^2 T W^3} \frac{1+2SNR}{SNR^2} \tag{4.25}$$

where, T is acquisition interval, W is the bandwidth of the signal, the SNR between the signal with power σ_s^2 and the ambient noise with variance σ_n^2 is defined as $SNR = \frac{\sigma_s^2}{\sigma_n^2}$. In order to transform discrete time, the signal is sampled with f_s. Then the time delay equals $\Delta = \Delta_t f_s$ is determined. Δ_t is the time delay in continuous time. Thus the CRLB in discrete-time is defined as,

$$CRLB(\Delta) = f_s^2 \; CRLB(\Delta_t) \tag{4.26}$$

The bandwidth of the signal is chosen as $f_s = 4W$ in simulations. So, inserting $f_s = 4W$ into (4.25) and (4.26),

$$CRLB(\Delta) = \frac{12}{\pi^2 T f_s} \frac{1+2SNR}{SNR^2} \tag{4.27}$$

Finally, the number of samples (N) equals $N = Tf_s$ and the final CRLB expression is given as,

$$CRLB(\Delta) = \frac{12}{\pi^2 N} \; \frac{1+2SNR}{SNR^2} \tag{4.28}$$

4.4. Simulation Results

In this section, two different estimation performances of the proposed method are given in order to see the effect of the estimating **R** matrices. We used two approaches in order to estimate the sample **R** matrix as mentioned previously. Thus, the TDOA estimation performances of the proposed BCFB based and ISSP based estimation methods are given in simulations. Besides, the estimation performance of the proposed method is compared with the CRLB. The performance criterion is the root-mean square error (RMSE) which is defined as following,

$$RMSE = \sqrt{E\{(\hat{\Delta} - \Delta)^2\}}$$

where, $\hat{\Delta}$ is the estimated value and the Δ is the exact value.

In simulations, a chirp signal is used as a wideband signal. The time duration of the signal is 0.1 sec. The bandwidth of the signal is $W = 250$ kHz and the sampling frequency is chosen as 1 MHz. The source is located at (4000, 4000). The reference sensor is located at (0, 0) and the second sensor is located at (100, 0). The simulation results are determined by 1000 independent Monte Carlo trials.

The two independent estimation performances of the proposed method are shown in simulations. This is because the spatial covariance matrices are estimated in two different ways. The first approach is based on ISSP. The number of blocks in (4.8) is selected as $B = 200$ and each block has 500 samples. The number of DFT points in each block is also 500. The second proposed approach is based on BCFB method and the parameters in (4.9) are selected as $P = 80$ and $L = 312$.

Figure 4.4. shows the estimation errors of the proposed estimator using BCFB which is proposed and the ISSP approaches. The estimation performances of the two estimators are also compared to the CRLB which shows the physical lower bound on variance of the estimators. As seen in the fig-

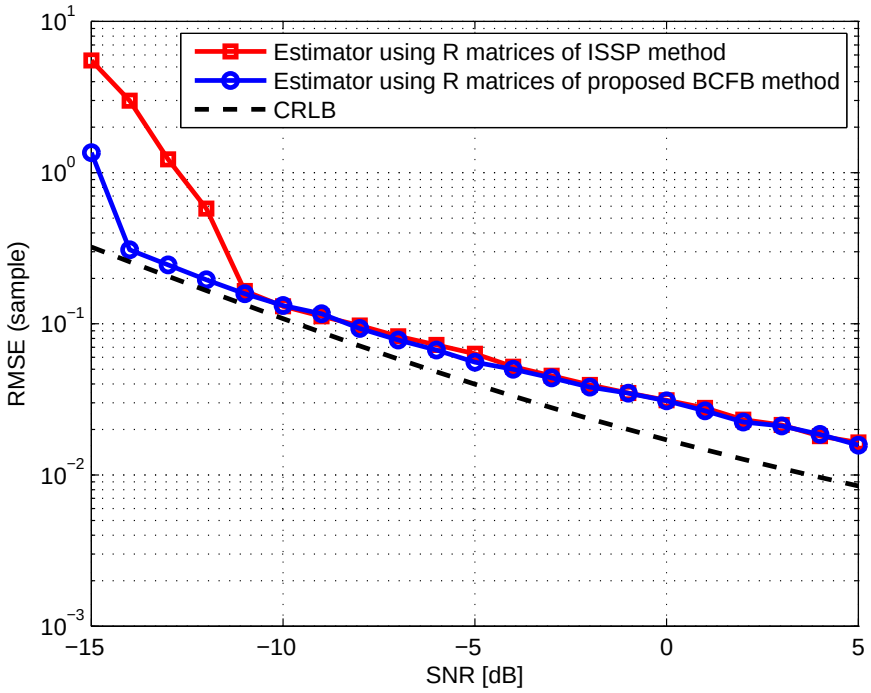

Figure 4.4.: The effect of the **R** matrix estimation to the estimation performance. The CRLB is given for comparison.

ure, the proposed BFCB based estimator goes along with the CRLB when the SNR is higher than -14 dB. Using the BCFB method improves the estimation performance especially in low SNR. In quite low SNR (below -14 dB), the performance of the estimator diverges from the CRLB depending on the noise effect. And there is also that, the estimator using ISSP method deviates from the estimator using BFCB and the CRLB when the SNR is below -11 dB.

In Figure 4.5., the estimation performances of the proposed estimator using BCFB to estimate **R** matrices according to sparsity level are shown. Sparsity level changes according to the parameters in (4.10). In figure, depending on the value of L, the sparsity level of the used data is determined and the estimation performances vary. As shown in figure, the best performance is obtained when the full data is used. With the increasing of sparsity level, the estimator performance degrades especially in quite low SNR (below -12 dB). When the amount of the used data drops under a definite level (in

%70 sparsity case), the estimation performance is affected. Concordantly, the system has much more computational cost when the used data increases. This is an undesired case in real time applications.

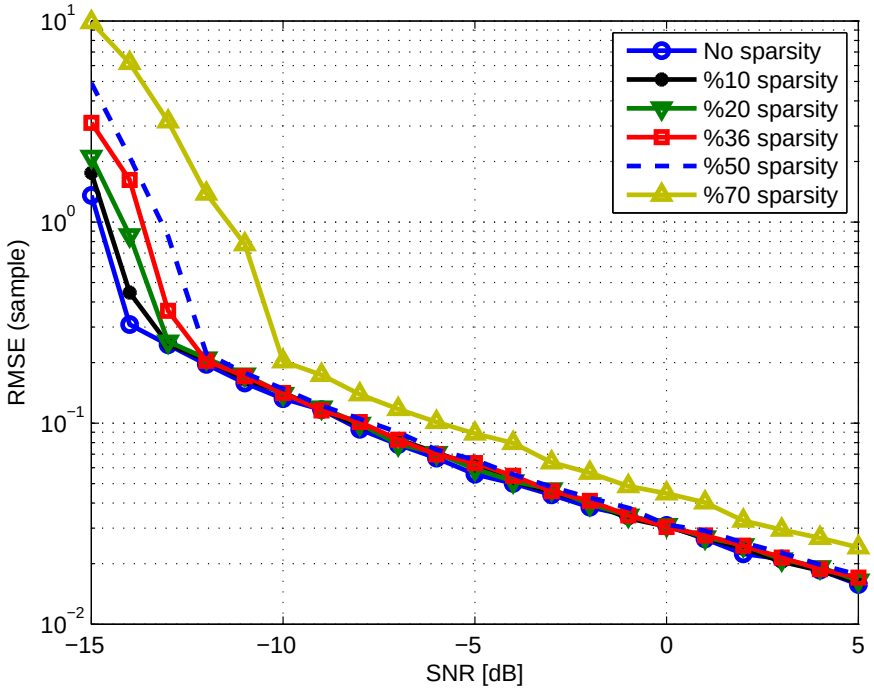

Figure 4.5.: The RMSE of the estimator according to the sparsity level.

Figure 4.6. shows the RMSE of the proposed estimator for the DS-SS signal according to the sparsity level. As seen in the figure, the TDOA estimator works for the DS-SS signals even in quite low SNR. The frequency components in the signal bandwidth is fully and sparsely used. The estimator performances in the form of two usage of the frequency data are close to each other up to -5 dB. When the SNR decreases below -5 dB, the estimator used sparse signal experiences a loss of performance. The estimator used a signal without sparsity performs close to the CRLB as shown in figure.

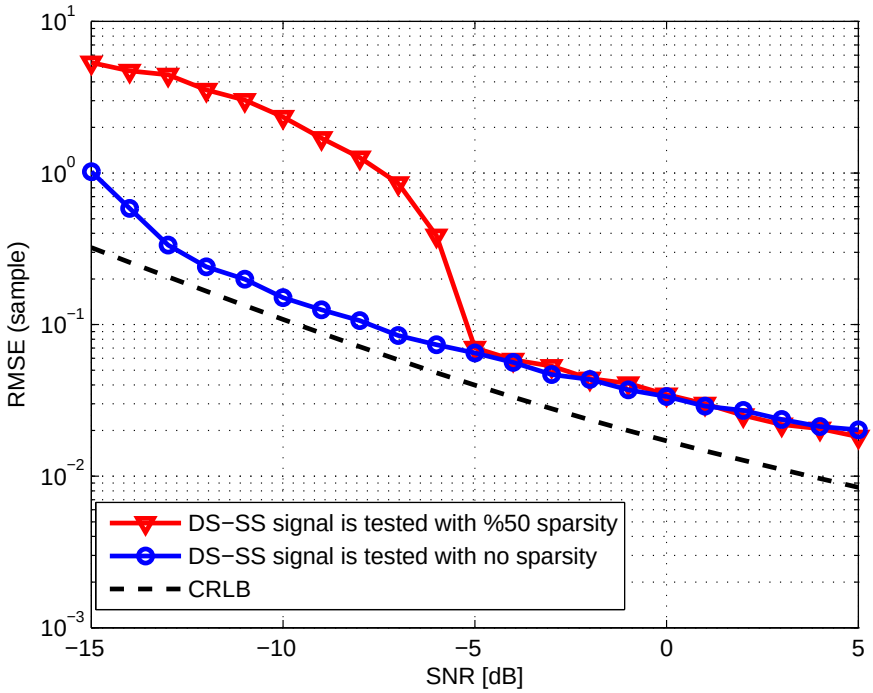

Figure 4.6.: The RMSE of the estimator for the DS-SS signal according to the sparsity level. The CRLB is also given for comparison.

4.5. Conclusion

In this section, a frequency domain TDOA estimator is proposed and the estimation performances in terms of root mean square error are given for various SNR cases. In order to estimate TDOA, the proposed method uses the phase slope of the estimated sample covariance matrices. In simulations, the proposed estimator is tested for the chirp signals and also for the DS-SS signals. In order to estimate sample covariance matrices, two different methods are used, the ISSP method and the proposed BCFB method. The ISSP is a well-known wideband signal processing method and the BCFB method is proposed in this thesis. In the BCFB method, the frequency components in the signal bandwidth is fully or sparsely utilized. The computational cost is reduced by using the sparse $\mathbf{R}$ matrices which is suitable for practical real time applications. The simulation results show that the proposed estimator

can estimate the TDOA in quite low SNR and it attains to the CRLB. In simulations, two sensors are used but it is possible to increase the number of sensors in array. In this case, the signal subspace based MUSIC or Root-MUSIC algorithms can be used to estimate cross phase terms.

5. CONCLUSION

In this thesis, the presence detection and TDOA estimation of direct sequence spread spectrum (DS-SS) signals are presented. In the first part of the thesis, the presence detection of DS-SS signals in white Gaussian noise is investigated by using a spatially distributed wideband sensor array. The presence detectors determines whether a signal is present or not. For the presence detection of both the long and short code DS-SS signals, two different multichannel methods are proposed. The first proposed detection method uses the phase slope of the cross channel terms of the spatial covariance matrices along the signal bandwidth. The normalized total root mean square error ($Total_{RMSE}$) is used as the test statistic for the signal detection. It is shown in simulations that the detection performance of the first proposed method is invariant from the spreading code length. It is also shown, it is possible to detect DS-SS signals in the presence of narrowband interferences and multipath reflections. The second proposed detection method is based on the eigenvalue ratio of the spatial covariance matrices. In addition, a new sample spatial covariance matrix ($\mathbf{R}$) estimation technique, which is called as block of consecutive frequency bins (BCFB), is proposed. In this technique, the sample covariance matrices are estimated in a sparse structure. Therefore, the proposed BCFB method is not requiring the whole frequency components of the signal. Also the BCFB method gives a stable $\mathbf{R}$ estimate especially in low SNR. It is shown that using the sample covariance matrix of the proposed BCFB method improves the detection performance especially in low SNR. It is also shown in various simulations that the proposed methods can detect the DS-SS signals in a stable way in quite low SNR without any prior information and assumption on target signal.

In the second part of the thesis, a frequency domain TDOA estimator is proposed for the DS-SS signals. TDOA of the received signals is estimated using only the phase slope of the estimated $\mathbf{R}$ matrices in the first proposed detection method. In this way, by using the proposed the sensors and hence

the location of the target signal. In simulations, the estimation performances in terms of root mean square error are given for various SNR levels. It is also shown that the proposed TDOA estimator's performance is efficient in low SNR and it attains to the Cramer Rao Lower Bound (CRLB).

REFERENCES

[1] R. Ziemer, *Fundamentals of Spread Spectrum Modulation*. Synthesis lectures on communications, Morgan & Claypool Publishers, 2007.

[2] M. Sharawi and D. Marko, "An introduction to direct-sequence spread-spectrum communications," *Oakland University, Rochester, Michigan*, 2000.

[3] R. L. Pickholtz, D. L. Schilling, and L. B. Milstein, "Theory of spread-spectrum communications–a tutorial," *Communications, IEEE Transactions on*, vol. 30, no. 5, pp. 855–884, 1982.

[4] V. Ipatov, *Spread Spectrum and CDMA: Principles and Applications*. John Wiley & Sons, 2005.

[5] *The ARRL Spread Spectrum Sourcebook*. Radioamatørernes Forlag, 1991.

[6] R. A. Scholtz, "The origins of spread-spectrum communications," *IEEE Transactions on Communications*, vol. 30, pp. 822–854, 1982.

[7] R. A. Dillard, "Detectability of spread-spectrum signals," *Aerospace and Electronic Systems, IEEE Transactions on*, no. 4, pp. 526–537, 1979.

[8] R. Dixon, *Spread spectrum systems*. Wiley-Interscience publication, J. Wiley, 1984.

[9] R. Gold, "Optimal binary sequences for spread spectrum multiplexing (corresp.)," *Information Theory, IEEE Transactions on*, vol. 13, no. 4, pp. 619–621, 1967.

[10] R. Dixon, *Spread Spectrum Techniques*. I E E E Press Selected Reprint Series, John Wiley & Sons Canada, Limited, 1976.

[11] A. Viterbi and J. Omura, *Principles of digital communication and coding*. McGraw-Hill series in electrical engineering, McGraw-Hill, 1979.

[12] D. L. Schilling, R. L. Pickholtz, and L. B. Milstein, "Spread spectrum goes commercial," *Spectrum, IEEE*, vol. 27, no. 8, pp. 40–41, 1990.

[13] E. Kaplan, "Signal-detection studies, with applications," *Bell System Technical Journal*, vol. 34, no. 2, pp. 403–437, 1955.

[14] H. Urkowitz, "Energy detection of unknown deterministic signals," *Proceedings of the IEEE*, vol. 55, no. 4, pp. 523–531, 1967.

[15] A. Sonnenschein and P. M. Fishman, "Radiometric detection of spread-spectrum signals in noise of uncertain power," *Aerospace and Electronic Systems, IEEE Transactions on*, vol. 28, no. 3, pp. 654–660, 1992.

[16] J. Lehtomaki, M. Juntti, H. Saarnisaari, and S. Koivu, "Threshold setting strategies for a quantized total power radiometer," *IEEE Signal Processing Letters*, vol. 12, no. 11, p. 796, 2005.

[17] W. A. Gardner and C. M. Spooner, "Signal interception: performance advantages of cyclic-feature detectors," *Communications, IEEE Transactions on*, vol. 40, no. 1, pp. 149–159, 1992.

[18] D. A. Hill and J. B. Bodie, "Carrier detection of psk signals," *Communications, IEEE Transactions on*, vol. 49, no. 3, pp. 487–496, 2001.

[19] J. F. Kuehls and E. Geraniotis, "Presence detection of binary-phase-shift-keyed and direct-sequence spread-spectrum signals using a prefilter-delay-and-multiply device," *Selected Areas in Communications, IEEE Journal on*, vol. 8, no. 5, pp. 915–933, 1990.

[20] M. K. Tsatsanis and G. B. Giannakis, "Blind estimation of direct sequence spread spectrum signals in multipath," *Signal Processing, IEEE Transactions on*, vol. 45, no. 5, pp. 1241–1252, 1997.

[21] W. A. Gardner, A. Napolitano, and L. Paura, "Cyclostationarity: Half a century of research," *Signal processing*, vol. 86, no. 4, pp. 639–697, 2006.

[22] G. Burel, C. Bouder, and O. Berder, "Detection of direct sequence spread spectrum transmissions without prior knowledge," in *Global Telecommunications Conference, 2001. GLOBECOM'01. IEEE*, vol. 1, pp. 236–239, IEEE, 2001.

[23] J. Yan and J. Hongbing, "A cyclic-cumulant based method for ds-ss signal detection and parameter estimation," in *Microwave, Antenna, Propagation and EMC Technologies for Wireless Communications, 2005. MAPE 2005. IEEE International Symposium on*, vol. 2, pp. 966–969, IEEE, 2005.

[24] T. Fusco, L. Izzo, A. Napolitano, and M. Tanda, "On the second-order cyclostationarity properties of long-code ds-ss signals," *Communications, IEEE Transactions on*, vol. 54, no. 10, pp. 1741–1746, 2006.

[25] D. J. Torrieri, "Performance of direct-sequence systems with long pseudonoise sequences," *Selected Areas in Communications, IEEE Journal on*, vol. 10, no. 4, pp. 770–781, 1992.

[26] R. S. Lunayach, "Performance of a direct sequence spread-spectrum system with long period and short period code sequences," *IEEE Transactions on Communications*, vol. 31, pp. 413–419, 1983.

[27] P.-Y. Qui, Z.-T. Huang, W.-L. Jiang, and C. Zhang, "Improved blind-spreading sequence estimation algorithm for direct sequence spread spectrum signals," *IET signal processing*, vol. 2, no. 2, pp. 139–146, 2008.

[28] H. Zhang, L. Gan, H. Liao, P. Wei, and L. Li, "Estimating spreading waveform of long-code direct sequence spread spectrum signals at a low signal-to-noise ratio," *Signal Processing, IET*, vol. 6, no. 4, pp. 358–363, 2012.

[29] S. Ghavami and B. Abolhassani, "Blind detection of ds-ss signals over fading channels using negentropy or kurtosis without any prior knowledge," in *Signal Processing and Information Technology, 2007 IEEE International Symposium on*, pp. 329–333, IEEE, 2007.

[30] Z. Deng, L. Shen, N. Bao, B. Su, J. Lin, and D. Wang, "Autocorrelation based detection of dsss signal for cognitive radio system," in *Wireless Communications and Signal Processing (WCSP), 2011 International Conference on*, pp. 1–5, IEEE, 2011.

[31] E. Adams and P. Hill, "Detection of direct sequence spread spectrum signals using higher-order statistical processing," in *Acoustics, Speech, and Signal Processing, IEEE International Conference on*, vol. 5, pp. 3849–3849, IEEE Computer Society, 1997.

[32] A. Momen, H. Ahmadi, and A. Mirzaee, "A new method in spread spectrum signal detection based on wavelet transform," in *Wireless and Optical Communications Networks, 2005. WOCN 2005. Second IFIP International Conference on*, pp. 600–602, IEEE, 2005.

[33] Y. Zhang and M. G. Amin, "Array processing for nonstationary interference suppression in ds/ss communications using subspace projection

techniques," *Signal Processing, IEEE Transactions on*, vol. 49, no. 12, pp. 3005–3014, 2001.

[34] G. Burel and C. Bouder, "Blind estimation of the pseudo-random sequence of a direct sequence spread spectrum signal," in *MILCOM 2000. 21st Century Military Communications Conference Proceedings*, vol. 2, pp. 967–970, IEEE, 2000.

[35] R. Madyasta and B. Aazhang, "Synchronization and detection of spread spectrum signals in multipath channels using antenna arrays," in *Military Communications Conference, 1995. MILCOM'95, Conference Record, IEEE*, vol. 3, pp. 1170–1174, IEEE, 1995.

[36] U. Ahnström, J. Falk, P. Händel, and M. Wikström, "Detection and direction-finding of spread spectrum signals using correlation and narrowband interference rejection," in *Nordic Matlab Conference*, 2003.

[37] C. Uysal and T. Filik, "Presence detection of long-and-short-code ds-ss signals using the phase linearity of multichannel sensors," in *Digital Signal Processing (DSP), 2014 19th International Conference on*, pp. 305–309, IEEE, 2014.

[38] C. Uysal and T. Filik, "Detection of low probability of intercept signals in low snr using multichannel sensor arrays," in *Signal Processing and Communications Applications Conference (SIU), 2014 22nd*, pp. 1845–1848, IEEE, 2014.

[39] M. Abu-Rgheff, *Introduction to CDMA Wireless Communications*. Elsevier Science, 2007.

[40] D. Torrieri, *Principles of Spread-Spectrum Communication Systems*. Springer, 2006.

[41] A. Viterbi, *CDMA: Principles of Spread Spectrum Communication*. Addison-Wesley wireless communications series, Addison-Wesley Publishing Company, 1995.

[42] P. Qiu, Z. Huang, W. Jiang, and C. Zhang, "Blind classification of the short-code and the long-code direct sequence spread spectrum signals," *Signal Processing, IET*, vol. 4, no. 1, pp. 78–88, 2010.

[43] H. Zhang, P. Wei, and Q. Mou, "A semidefinite relaxation approach to blind despreading of long-code ds-ss signal with carrier frequency offset," *Signal Processing Letters, IEEE*, vol. 20, no. 7, pp. 705–708, 2013.

[44] A. Piersol, "Time delay estimation using phase data," *Acoustics, speech and signal processing, IEEE Transactions on*, vol. 29, no. 3, pp. 471–477, 1981.

[45] Y.-S. Yoon, L. M. Kaplan, and J. H. McClellan, "Tops: new doa estimator for wideband signals," *Signal Processing, IEEE Transactions on*, vol. 54, no. 6, pp. 1977–1989, 2006.

[46] W. Ng, J. P. Reilly, T. Kirubarajan, and J.-R. Larocque, "Wideband array signal processing using mcmc methods," *Signal Processing, IEEE Transactions on*, vol. 53, no. 2, pp. 411–426, 2005.

[47] M. Zatman, "How narrow is narrowband?," *IEE Proceedings-Radar, Sonar and Navigation*, vol. 145, no. 2, pp. 85–91, 1998.

[48] M. Wax, T.-J. Shan, and T. Kailath, "Spatio-temporal spectral analysis by eigenstructure methods," *IEEE Transactions on Acoustics Speech and Signal Processing*, vol. 32, pp. 817–827, 1984.

[49] J. Chen, J. Benesty, and Y. A. Huang, "Time delay estimation in room acoustic environments: an overview," *EURASIP Journal on Advances in Signal Processing*, vol. 2006, 2006.

[50] A. N. Bishop, B. Fidan, B. Anderson, K. Dogancay, and P. N. Pathirana, "Optimal range-difference-based localization considering geometrical constraints," *Oceanic Engineering, IEEE Journal of*, vol. 33, no. 3, pp. 289–301, 2008.

[51] A. Amar and A. J. Weiss, "Localization of narrowband radio emitters based on doppler frequency shifts," *Signal Processing, IEEE Transactions on*, vol. 56, no. 11, pp. 5500–5508, 2008.

[52] M. C. Vanderveen, A.-J. Van der Veen, and A. Paulraj, "Estimation of multipath parameters in wireless communications," *Signal Processing, IEEE Transactions on*, vol. 46, no. 3, pp. 682–690, 1998.

[53] J. C. Hassab, *Underwater signal and data processing*. CRC Press Boca

Raton, FL, 1989.

[54] Y. Huang, J. Benesty, and G. W. Elko, "Adaptive eigenvalue decomposition algorithm for real time acoustic source localization system," in *Acoustics, Speech, and Signal Processing, 1999. Proceedings., 1999 IEEE International Conference on*, vol. 2, pp. 937–940, IEEE, 1999.

[55] J. Benesty, "Adaptive eigenvalue decomposition algorithm for passive acoustic source localization," *The Journal of the Acoustical Society of America*, vol. 107, no. 1, pp. 384–391, 2000.

[56] S. Doclo and M. Moonen, "Robust adaptive time delay estimation for speaker localization in noisy and reverberant acoustic environments," *EURASIP Journal on Advances in Signal Processing*, vol. 2003, no. 11, pp. 1110–1124, 1900.

[57] T. G. Dvorkind and S. Gannot, "Time difference of arrival estimation of speech source in a noisy and reverberant environment," *Signal Processing*, vol. 85, no. 1, pp. 177–204, 2005.

[58] Y. Huang, J. Benesty, G. W. Elko, and R. M. Mersereati, "Real-time passive source localization: A practical linear-correction least-squares approach," *Speech and Audio Processing, IEEE Transactions on*, vol. 9, no. 8, pp. 943–956, 2001.

[59] W. H. Foy, "Position-location solutions by taylor-series estimation," 1976.

[60] M. Wax and T. Kailath, "Optimum localization of multiple sources by passive arrays," *Acoustics, Speech and Signal Processing, IEEE Transactions on*, vol. 31, no. 5, pp. 1210–1217, 1983.

[61] K. Dogançay, "Emitter localization using clustering-based bearing association," *Aerospace and Electronic Systems, IEEE Transactions on*, vol. 41, no. 2, pp. 525–536, 2005.

[62] R. O. Schmidt, "A new approach to geometry of range difference location," 1972.

[63] J. A. Smith *et al.*, "closed-form. least-squares source location estimation from range-difference measurements," 1987.

[64] H. Schau and A. Robinson, "Passive source localization employing in-

tersecting spherical surfaces from time-of-arrival differences," *Acoustics, Speech and Signal Processing, IEEE Transactions on*, vol. 35, no. 8, pp. 1223–1225, 1987.

[65] M. D. Gillette and H. F. Silverman, "A linear closed-form algorithm for source localization from time-differences of arrival," *Signal Processing Letters, IEEE*, vol. 15, pp. 1–4, 2008.

[66] A. Masmoudi, F. Bellili, S. Affes, and A. Stephenne, "A maximum likelihood time delay estimator in a multipath environment using importance sampling," *Signal Processing, IEEE Transactions on*, vol. 61, no. 1, pp. 182–193, 2013.

[67] C. Knapp and G. C. Carter, "The generalized correlation method for estimation of time delay," *Acoustics, Speech and Signal Processing, IEEE Transactions on*, vol. 24, no. 4, pp. 320–327, 1976.

[68] T. G. Manickam, R. J. Vaccaro, and D. W. Tufts, "A least-squares algorithm for multipath time-delay estimation," *Signal Processing, IEEE Transactions on*, vol. 42, no. 11, pp. 3229–3233, 1994.

[69] M. Wax, "The joint estimation of differential delay, doppler, and phase (corresp.)," *Information Theory, IEEE Transactions on*, vol. 28, no. 5, pp. 817–820, 1982.

[70] Y. Chan, R. Hattin, and J. Plant, "The least squares estimation of time delay and its use in signal detection," in *Acoustics, Speech, and Signal Processing, IEEE International Conference on ICASSP'78.*, vol. 3, pp. 665–669, IEEE, 1978.

[71] Y. Huang, J. Lin, and M. Giess, "High accuracy time delay measurements for band-pass signals," 2013.

[72] A. Masmoudi, F. Bellili, S. Affes, and A. Stephenne, "A non-data-aided maximum likelihood time delay estimator using importance sampling," *Signal Processing, IEEE Transactions on*, vol. 59, no. 10, pp. 4505–4515, 2011.

[73] H. He, L. Wu, J. Lu, X. Qiu, and J. Chen, "Time difference of arrival estimation exploiting multichannel spatio-temporal prediction," *Audio,*

Speech, and Language Processing, IEEE Transactions on, vol. 21, no. 3, pp. 463–475, 2013.

[74] R. O. Schmidt, "Multiple emitter location and signal parameter estimation," *Antennas and Propagation, IEEE Transactions on*, vol. 34, no. 3, pp. 276–280, 1986.

[75] A. Barabell, "Improving the resolution performance of eigenstructure-based direction-finding algorithms," in *Acoustics, Speech, and Signal Processing, IEEE International Conference on ICASSP'83.*, vol. 8, pp. 336–339, IEEE, 1983.

[76] B. Friedlander, "The root-music algorithm for direction finding with interpolated arrays," *Signal Processing*, vol. 30, no. 1, pp. 15–29, 1993.

[77] H. L. Van Trees, "Optimum array processing (detection, estimation, and modulation theory, part iv)," *John Wiley and Sons Inc., New York*, vol. 65, pp. 3185–3201, 2002.

[78] J. M. Bioucas-Dias and G. Valadão, "Phase unwrapping via graph cuts," *Image Processing, IEEE Transactions on*, vol. 16, no. 3, pp. 698–709, 2007.

[79] G. C. Carter, "Coherence and time delay estimation," *Proceedings of the IEEE*, vol. 75, no. 2, pp. 236–255, 1987.

[80] J. Falk, "An electronic warfare perspective on time difference of arrival estimation subject to radio receiver imperfections licentiate thesis," *Royal Institute of Technology, Stockholm, Sweden*, vol. 2, 2004.